MOX–Report No. 20/2008

Model adaptation enriched with an anisotropic mesh spacing for advection-diffusion-reaction systems

Filippo David, Stefano Micheletti, Simona Perotto

MOX, Dipartimento di Matematica "F. Brioschi"
Politecnico di Milano, Via Bonardi 29 - 20133 Milano (Italy)

mox@mate.polimi.it http://mox.polimi.it

Model adaptation enriched with an anisotropic mesh spacing for advection-diffusion-reaction systems*

Filippo David†, Stefano Micheletti♯ and Simona Perotto♯

11 Settembre 2008

† STMicroelectronics
Via Tolomeo 1, I-20100 Cornaredo (MI), Italy
filippo.david@st.com

♯ MOX– Modellistica e Calcolo Scientifico
Dipartimento di Matematica "F. Brioschi"
Politecnico di Milano
via Bonardi 9, I-20133 Milano, Italy
{stefano.micheletti,simona.perotto}@polimi.it

Keywords: model adaptivity, anisotropic mesh adaptation, goal-oriented analysis, advection-diffusion-reaction systems, finite elements

AMS Subject Classification: 65N15, 65N50, 65J15, 35J60

Abstract

We propose a procedure aiming at reducing the computational cost involved in the numerical approximation of (possibly nonlinear) advection-diffusion-reaction systems. The idea is to suitably combine a model with a mesh adaptive procedure. In particular we first derive, separately, a model error estimator and an anisotropic estimator for the discretization error, suited for driving a model and a mesh adaptivity algorithm, respectively. These two strategies are then properly combined, allowing for a merged model-mesh control. The whole procedure is finally assessed on some numerical test cases, essentially inspired by ecological and environmental applications.

1 Introduction and motivations

Many of the problems of interest in Applied Sciences involve different temporal and spatial scales as well as physical phenomena of different nature, often limited to some portion of the whole computational domain. This issue, for instance, is typical when monitoring the concentration of some pollutant in a river or in air, rather than when interested in the fluid-dynamics in a river with obstacles,

*This research was supported by PRIN 2006 "Approssimazione Numerica di Problemi Multiscala e Multifisica con Tecniche Adattive".

as well as if dealing with the measurement of a solute concentration in a blood vessel, or of the electric current at the terminals of a semiconductor electronic device.
With a view to the numerical simulation of such phenomena, *mesh adaptivity* plays an important role to manage the coexistence of different time and space scales. The idea is to reduce the involved computational costs by selecting small mesh spacing and time step only where and when strictly necessary. As a matter of fact, mesh adaptive procedures have been actively investigated for the numerical approximation of PDE's models since the late '70s (see, e.g., [4, 5, 53, 8, 7, 51]) and are standard tools in most of the main commercial softwares.

On the other hand, the dominance of some physical features in restricted areas of the domain suggests giving up the employment of the full model on the whole domain, locally replaced by a simpler model. This philosophy has led to the more recent *model adaptation*. This approach covers distinct frameworks: for instance the heterogeneous domain decomposition method matches different boundary value problems associated with disjoint subregions of the computational domain (see, e.g., [45]); the geometric multiscale strategy couples models characterized by a different spatial dimension (see, e.g., [21]); the hierarchical model reduction combines models with the same dimension but exhibiting a different level of accuracy in describing the phenomenon at hand (see, e.g., [52, 1, 6, 19]).

In this paper we resort to an alternative technique. The idea is to merge the full model with a reduced counterpart, obtained by dropping in the full model the most expensive term from the computational viewpoint. For example, in the case of an advection-diffusion problem, the advective term (the most troublesome to deal with numerically) may be relevant (and thus included in the model) just in a small part of the domain. This approach has been proposed in a goal-oriented framework by, e.g., [38, 10]. A successive variant is provided in [43] and applied to the approximation of the unsteady shallow water equations. The present work aims at enriching the analysis in [43] with a suitable mesh adaptation procedure, our reference full model being a general (possibly nonlinear) advection-diffusion-reaction system. The combination of mesh and model adaptivity is not often tackled in the literature (see, e.g., [10, 11, 49]). Our goal is to further lighten the computational cost of a model-mesh adaptive procedure by advocating an anisotropic mesh adaptation strategy (see, e.g., [13, 27, 18, 2, 16, 22, 48, 50, 44, 25, 28]). This turns out to be particularly convenient in the presence of strongly directional features, such as the ones induced by a dominant advection.

The outline of the paper is the following one: We first focus on the model adaptation only. In particular, Section 2 faces the linear case, while in Section 3 we deal with the nonlinear framework. In Section 4 we move to the mesh adaptation by introducing the anisotropic setting, as well as a goal-oriented anisotropic a posteriori analysis. Finally, in Section 5 the model and mesh adaptivities are merged. The numerical test cases throughout the paper are both academic and inspired by ecological and environmental applications.

2 An a posteriori model analysis: the linear case

Aim of this section is to provide an a posteriori model error analysis for a general linear variational problem. The idea is to be free from the Lagrangian approach typical of the nonlinear case (see, e.g., [10, 11, 38, 39, 40, 41, 43]). Thus we are led to a simplified setting, still hinging on the dual framework with a view to a goal-oriented error control (see, e.g., [9, 26, 30, 37]). The proposed analysis also includes the treatment of nonhomogeneous Dirichlet boundary conditions as well as a Petrov-Galerkin formulation for both the primal and dual problems. Let V and W be two real Hilbert spaces associated with the computational domain $\Omega \subset \mathbb{R}^2$, and $V_0 \subseteq V, W_0 \subseteq W$ be two corresponding subspaces. Let $c \in V$ and $g \in W$ be two fixed elements, related to the nonhomogeneous Dirichlet data. Let us introduce the general linear problem to be approximated: find $u_1 \in V_0 + c$ s.t.

$$a(u_1, w) + d(u_1, w) = F(w) \quad \forall w \in W_0, \tag{1}$$

where $a(\cdot,\cdot)$, $d(\cdot,\cdot)$ are bilinear forms defined on $V \times W$ and $F : W \to \mathbb{R}$ is a linear functional, possibly accounting for nonhomogeneous Neumann conditions. Standard regularity assumptions are made on the problem data so that (1) is well-posed. Notice the different function spaces employed for the solution and the test function in the spirit of a Petrov-Galerkin formulation, $V_0 + c \subseteq V$ being an affine space. Moreover we assume that the bilinear form $d(\cdot,\cdot)$ gathers the most expensive part involved in the computation of (1).
Throughout the paper we refer to (1) as to the *fine primal problem*.

The actual goal is to estimate $J_{goal}(u_1)$, where $J_{goal} : V \to \mathbb{R}$ is a linear functional of interest identifying a certain physically meaningful quantity (see Sections 2.2 and 3.1 for possible instances).
In particular we suppose to deal with physical problems where the influence of the bilinear form $d(\cdot,\cdot)$ on the estimation of $J_{goal}(u_1)$ is confined to small portions of Ω. The idea is to propose an automatic tool able to detect these areas (Ω_1) of influence in order to contain the involved computational cost with respect to the employment of the fine model on the whole Ω. We are thus led to solve a variational problem where $d(\cdot,\cdot)$ contributes only "spotwise" or, likewise, on certain regions (Ω_0) of Ω we solve the so-called *coarse problem* identified by the sole bilinear form $a(\cdot,\cdot)$.
For this purpose we introduce the *adapted primal problem*: find $u_\alpha \in V_0 + c$ s.t.

$$a(u_\alpha, w) + d(u_\alpha, \alpha w) = F(w) \quad \forall w \in W_0, \tag{2}$$

where $\alpha \in L^\infty(\Omega)$ takes on only the values 0 or 1. When $\alpha = 0$ everywhere we get the coarse model, whereas we recover (1) for $\alpha = 1$ on the whole Ω. In the general case none of these two situations occurs. On the contrary, the choice $\alpha = \chi_{\Omega_1}$ yields a possible adapted model, the one to be actually solved, χ denoting the characteristic function.
We point out that the second argument of $d(\cdot,\cdot)$ must not depend on any derivative, due to the regularity of α. Moreover, the form $d(\cdot,\cdot)$ must not change the differential nature (elliptic, hyperbolic, etc) of the coarse problem associated with the bilinear form $a(\cdot,\cdot)$.

With the aim of a goal-oriented analysis we define the *fine dual problem*

associated with the primal one (1): find $z_1 \in W_0 + g$ s.t.

$$a(v, z_1) + d(v, z_1) = J(v) \quad \forall v \in V_0, \tag{3}$$

where $W_0 + g \subseteq W$ is an affine space of W while $J : V \to \mathbb{R}$ is a suitable linear functional which will be related to J_{goal} at the end of this section. Likewise we introduce the *adapted dual problem*: find $z_\alpha \in W_0 + g$ s.t.

$$a(v, z_\alpha) + d(v, \alpha z_\alpha) = J(v) \quad \forall v \in V_0. \tag{4}$$

To make the analysis below more straightforward we rewrite the primal and dual problems above by exploiting the splitting $u_\alpha = \widetilde{u}_\alpha + c$, $z_\alpha = \widetilde{z}_\alpha + g$, with $\widetilde{u}_\alpha \in V_0$ and $\widetilde{z}_\alpha \in W_0$. This yields: find $\widetilde{u}_\alpha \in V_0$ s.t.

$$a(\widetilde{u}_\alpha, w) + d(\widetilde{u}_\alpha, \alpha\, w) = F(w) - a(c, w) - d(c, \alpha\, w) = \widetilde{F}_\alpha(w) \quad \forall w \in W_0 \tag{5}$$

with reference to problem (2); find $\widetilde{z}_\alpha \in W_0$ s.t.

$$a(v, \widetilde{z}_\alpha) + d(v, \alpha\, \widetilde{z}_\alpha) = J(v) - a(v, g) - d(v, \alpha\, g) = \widetilde{J}_\alpha(v) \quad \forall v \in V_0, \tag{6}$$

for problem (4). The choice $\alpha = 1$ in (5) and (6) yields the corresponding reformulations of (1) and (3), respectively.

We anticipate some preliminary results before focusing on the main estimate. We begin with proving the following *model orthogonalities*:

Lemma 2.1 *Let $\widetilde{e}_m = \widetilde{u}_1 - \widetilde{u}_\alpha = u_1 - u_\alpha$ and $\widetilde{e}^*_m = \widetilde{z}_1 - \widetilde{z}_\alpha = z_1 - z_\alpha$ be the primal and dual model error, respectively. Then it holds*

$$a(\widetilde{e}_m, w) + d(\widetilde{e}_m, w) + d(u_\alpha, (1-\alpha)\, w) = 0 \quad \forall w \in W_0; \tag{7}$$

$$a(v, \widetilde{e}^*_m) + d(v, \widetilde{e}^*_m) + d(v, (1-\alpha)\, z_\alpha) = 0 \quad \forall v \in V_0. \tag{8}$$

Proof. It follows on suitably subtracting the adapted formulations (5) and (6) from their corresponding fine counterparts. □

By mimicking the relation leading to result (1.8) in [9] we establish

Lemma 2.2 *The following relation links the primal with the dual model errors on $\widetilde{J}_1$ and $\widetilde{F}_1$:*

$$\widetilde{J}_1(\widetilde{e}_m) = \widetilde{F}_1(\widetilde{e}^*_m) + d(\widetilde{u}_\alpha, (1-\alpha)\, z_\alpha) - d(u_\alpha, (1-\alpha)\, \widetilde{z}_\alpha).$$

Proof. Choosing $v = \widetilde{e}_m$ in the dual problem (6) with $\alpha = 1$, exploiting the model orthogonalities (7) and (8) with $w = \widetilde{z}_\alpha$ and $v = \widetilde{u}_\alpha$, respectively, we get

$$\begin{aligned} \widetilde{J}_1(\widetilde{e}_m) &= a(\widetilde{e}_m, \widetilde{e}^*_m) + d(\widetilde{e}_m, \widetilde{e}^*_m) - d(u_\alpha, (1-\alpha)\, \widetilde{z}_\alpha) \\ &= a(\widetilde{u}_1, \widetilde{e}^*_m) + d(\widetilde{u}_1, \widetilde{e}^*_m) + d(\widetilde{u}_\alpha, (1-\alpha)\, z_\alpha) - d(u_\alpha, (1-\alpha)\, \widetilde{z}_\alpha). \end{aligned}$$

Finally the fine primal problem, i.e., (5) with $\alpha = 1$, for the choice $w = \widetilde{e}^*_m$ provides us with the desired result. □

Let us introduce the primal $\widetilde{\rho}(\widetilde{u}_\alpha, \cdot) : W_0 \to \mathbb{R}$ and the dual $\widetilde{\rho}^*(\cdot, \widetilde{z}_\alpha) : V_0 \to \mathbb{R}$ *model residuals* given by

$$\widetilde{\rho}(\widetilde{u}_\alpha, \cdot) = \widetilde{F}_1(\cdot) - a(\widetilde{u}_\alpha, \cdot) - d(\widetilde{u}_\alpha, \cdot), \quad \widetilde{\rho}^*(\cdot, \widetilde{z}_\alpha) = \widetilde{J}_1(\cdot) - a(\cdot, \widetilde{z}_\alpha) - d(\cdot, \widetilde{z}_\alpha), \tag{9}$$

respectively. These quantities measure the extent the adapted solutions $\widetilde{u}_\alpha$ and $\widetilde{z}_\alpha$ fail to satisfy the corresponding fine problems.
An equivalent expression for the residuals in (9) can be obtained via the following

Lemma 2.3 *It holds*

$$\widetilde{\rho}(\widetilde{u}_\alpha, \cdot) = -d(u_\alpha, (1-\alpha)\,\cdot), \quad \widetilde{\rho}^*(\cdot, \widetilde{z}_\alpha) = -d(\cdot, (1-\alpha)\, z_\alpha).$$

Proof. Using the definition $(9)_1$ and adding and subtracting $d(\widetilde{u}_\alpha, \alpha\, w)$ yields

$$\widetilde{\rho}(\widetilde{u}_\alpha, w) = \widetilde{F}_1(w) - a(\widetilde{u}_\alpha, w) - d(\widetilde{u}_\alpha, \alpha\, w) - d(\widetilde{u}_\alpha, (1-\alpha)\, w).$$

By relating $\widetilde{F}_1(w)$ to $\widetilde{F}_\alpha(w)$ via (5), we get

$$\widetilde{\rho}(\widetilde{u}_\alpha, w) = \widetilde{F}_\alpha(w) - d(c, (1-\alpha)\, w) - a(\widetilde{u}_\alpha, w) - d(\widetilde{u}_\alpha, \alpha\, w) - d(\widetilde{u}_\alpha, (1-\alpha)\, w).$$

The adapted primal formulation along with the splitting $u_\alpha = \widetilde{u}_\alpha + c$ provides us with the final result.
An analogous proof holds for the dual residual $\widetilde{\rho}^*(\cdot, \widetilde{z}_\alpha)$. □

Lemma 2.4 *The primal and dual model error on $\widetilde{J}_1$ and $\widetilde{F}_1$ can be expressed as*

$$\widetilde{J}_1(\widetilde{e}_m) = \min_{\varphi \in W_0} \Big\{ \widetilde{\rho}(\widetilde{u}_\alpha, \widetilde{z}_1 - \varphi) - d(u_\alpha, (1-\alpha)\, \varphi) \Big\}. \tag{10}$$

and

$$\widetilde{F}_1(\widetilde{e}^*_m) = \min_{\psi \in V_0} \Big\{ \widetilde{\rho}^*(\widetilde{u}_1 - \psi, \widetilde{z}_\alpha) - d(\psi, (1-\alpha)\, z_\alpha) \Big\}, \tag{11}$$

respectively.

Proof. Thanks to the fine dual problem for $v = \widetilde{e}_m$ and the model orthogonality (7) with $w = \varphi$, for any $\varphi \in W_0$, we have

$$\widetilde{J}_1(\widetilde{e}_m) = a(\widetilde{e}_m, \widetilde{z}_1) + d(\widetilde{e}_m, \widetilde{z}_1) = a(\widetilde{e}_m, \widetilde{z}_1 - \varphi) + d(\widetilde{e}_m, \widetilde{z}_1 - \varphi) - d(u_\alpha, (1-\alpha)\, \varphi).$$

The definition of the primal model error $\widetilde{e}_m$ combined with the fine primal problem for $w = \widetilde{z}_1 - \varphi$ yields

$$\widetilde{J}_1(\widetilde{e}_m) = \widetilde{F}_1(\widetilde{z}_1 - \varphi) - [a(\widetilde{u}_\alpha, \widetilde{z}_1 - \varphi) + d(\widetilde{u}_\alpha, \widetilde{z}_1 - \varphi)] - d(u_\alpha, (1-\alpha)\, \varphi).$$

The thesis follows recalling the definition of the primal model residual $(9)_1$ and from the arbitrariness of φ in W_0. Result (11) follows on suitably exchanging the role played by the primal and dual problems in the proof of (10). □

The main result of this section provides an estimate for the model error on $\widetilde{J}_1$ merging both the primal and dual contributions.

Proposition 2.1 *Let $\widetilde{u}_1$ and $\widetilde{u}_\alpha$ be the fine and the adapted primal solutions associated with (5) and $\widetilde{z}_1$ and $\widetilde{z}_\alpha$ the corresponding dual solutions. Let $\widetilde{e}_m$ and $\widetilde{e}^*_m$ be the primal and dual model errors as in Lemma 2.1. Then it holds*

$$\widetilde{J}_1(\widetilde{e}_m) = -d(u_\alpha, (1-\alpha)\, \widetilde{z}_\alpha) + \frac{1}{2}\Big[\widetilde{\rho}(\widetilde{u}_\alpha, \widetilde{e}^*_m) + \widetilde{\rho}^*(\widetilde{e}_m, \widetilde{z}_\alpha)\Big],$$

$\widetilde{\rho}(\widetilde{u}_\alpha, \cdot)$ and $\widetilde{\rho}^*(\cdot, \widetilde{z}_\alpha)$ being defined as in (9), and with u_α solution to (2).

Proof. We proceed with the trivial splitting $\widetilde{J}_1(\widetilde{e}_m) = \frac{1}{2}\widetilde{J}_1(\widetilde{e}_m) + \frac{1}{2}\widetilde{J}_1(\widetilde{e}_m)$. Then we employ (10) in Lemma 2.4 on the first term and Lemma 2.2 combined with (11) in Lemma 2.4 on the second one, for arbitrary $\varphi \in W_0$ and $\psi \in V_0$:

$$\begin{aligned} \widetilde{J}_1(\widetilde{e}_m) \;&=\; \tfrac{1}{2}\Big[\widetilde{\rho}(\widetilde{u}_\alpha, \widetilde{z}_1 - \varphi) - d(u_\alpha, (1-\alpha)\, \varphi)\Big] \\ &+\; \tfrac{1}{2}\Big[\widetilde{\rho}^*(\widetilde{u}_1 - \psi, \widetilde{z}_\alpha) - d(\psi, (1-\alpha)\, z_\alpha) + d(\widetilde{u}_\alpha, (1-\alpha)\, z_\alpha) - d(u_\alpha, (1-\alpha)\, \widetilde{z}_\alpha)\Big]. \end{aligned}$$

Now by suitably rearranging the terms on the right-hand side we have

$$\begin{aligned}\widetilde{J}_1(\widetilde{e}_m) &= \tfrac{1}{2}\Big[\widetilde{\rho}(\widetilde{u}_\alpha, \widetilde{z}_1 - \varphi) + \widetilde{\rho}^*(\widetilde{u}_1 - \psi, \widetilde{z}_\alpha)\Big] \\ &- \tfrac{1}{2}\Big[d(u_\alpha, (1-\alpha)\,\varphi) + d(\psi, (1-\alpha)\,z_\alpha) - d(\widetilde{u}_\alpha, (1-\alpha)\,z_\alpha) + d(u_\alpha, (1-\alpha)\,\widetilde{z}_\alpha)\Big],\end{aligned}$$

i.e., the final result after choosing $\varphi = \widetilde{z}_\alpha$ and $\psi = \widetilde{u}_\alpha$. □

Remark 2.1 *In a similar fashion we can prove the equality*

$$\widetilde{F}_1(\widetilde{e}_m^*) = -d(\widetilde{u}_\alpha, (1-\alpha)\,z_\alpha) + \frac{1}{2}\Big[\widetilde{\rho}(\widetilde{u}_\alpha, \widetilde{e}_m^*) + \widetilde{\rho}^*(\widetilde{e}_m, \widetilde{z}_\alpha)\Big].$$

With reference to Proposition 2.1 we highlight that only the first term on the right-hand side is fully computable whereas the second one depends (to first order accuracy) on both the primal and dual errors. Thus, with a view to the adaptive procedure in Section 2.1, we can introduce the *model error estimator* η_α for $\widetilde{J}_1(\widetilde{e}_m)$ given by

$$\eta_\alpha = -d(u_\alpha, (1-\alpha)\,\widetilde{z}_\alpha) \ \big(\equiv \widetilde{\rho}(\widetilde{u}_\alpha, \widetilde{z}_\alpha)\big). \tag{12}$$

As the actual goal is to estimate $J_{goal}(\widetilde{e}_m)$, it is convenient, in the light of Proposition 2.1, to choose $\widetilde{J}_1 = J_{goal}$. As a consequence the functional J in the fine dual problem (3) is given by $J(v) = J_{goal}(v) + a(v, g) + d(v, g)$.

2.1 The model adaptive procedure

We aim at devising a reliable iterative procedure, referred to as *model adaptation procedure*, able to "translate" the error estimator η_α in (12) into a practical criterion for selecting the fine (Ω_1) and coarse (Ω_0) areas in Ω.
With a view to the actual computation of the adapted problems (2) and (6), we introduce a conformal partition $\mathcal{T}_h = \{K\}$ of $\overline{\Omega}$ into N_h triangles K. At this stage we assume that $\mathcal{T}_h$ is sufficiently fine so that the discretization error is negligible.

To initiate the iterative procedure, we select reference primal and dual solutions computationally cheap, i.e., we let $u_\alpha = u_0$ and $\widetilde{z}_\alpha = \widetilde{z}_0$. This leads to identify the initial guess for the model error estimator with $\eta_0 = -d(u_0, \widetilde{z}_0)$, according to definition (12). The final goal of the procedure is to identify the suitable function $\alpha = \chi_{\Omega_1}$ so that $|J(u_1 - u_\alpha)| \leq \tau_m$, with τ_m a user-defined tolerance, and such that the measure of Ω_1 be as small as possible.

The main steps of the model adaptation algorithm are listed in the following α-`adaptive procedure`:

1. `set` $\alpha\big|_K = 0, \forall K \in \mathcal{T}_h$;

2. `solve (2) and (6);`

3. `compute` η_α `via (12);`

4. if $|\eta_\alpha| \leq \tau_m$ break

5. for i=1,$\mathtt{N_{max}}$

6. localize η_α on each $K \in \mathcal{T}_h$: $\eta_{\alpha,K} = \eta_\alpha\big|_K$;

7. if $|\eta_{\alpha,K}| > \delta \dfrac{\tau_m}{N_h}$, $\alpha\big|_K \leftarrow 1$;

8. solve (2) and (6);

9. compute η_α via (12);

10. if $|\eta_\alpha| \leq \tau_m$ break

end

The localization in step 6. simply relies on the additive property of the integrals defining the bilinear form $d(\cdot,\cdot)$. The check at step 7. is meant in the spirit of an equidistribution of the total model error over the triangles. This mimics what is typically done in the mesh adaptivity framework. Through the parameter $\delta > 1$ we aim at limiting the model refinement only to the "worst" elements. In practice this value is chosen so that, at each iteration, the variation of the fine area Ω_1 is at most the 5% of the whole area $|\Omega|$. The adopted criterion avoids the continuous switching on and off of the fine model in the same element caused by the factor $1-\alpha$ in (12).
Step 10. aims at guaranteeing the reliability of the estimator (12). Indeed η_α neglects the model residuals $\widetilde{\rho}(\widetilde{u}_\alpha, \widetilde{e}^*_m)$ and $\widetilde{\rho}^*(\widetilde{e}_m, \widetilde{z}_\alpha)$. Moreover since step 7. provides a "prediction" for a new distribution of the function α, we need to check the goodness of such a prediction via steps 8.-10..
Finally, to ensure the termination of the adaptive procedure in the case of a failure in satisfying the global tolerance, we have fixed a maximum number $\mathtt{N_{max}}$ of iterations.
We point out that the α-adaptive procedure is not guaranteed to be efficient, i.e., the area returned for Ω_1 is not necessarily a minimum. However both the choices made for the initial guess and the equidistribution criterion serve to meet this goal.

2.2 Some examples

We assess the reliability of the error estimator η_α in (12) as well as the efficiency of the α-adaptive procedure on the well-established scalar advection-diffusion-reaction (ADR) equation

$$\begin{cases} -\mu\Delta u + \mathbf{b}\cdot\nabla u + \sigma u = f & \text{in } \Omega, \\ u = c_1 & \text{on } \Gamma_D, \\ \mu\dfrac{\partial u}{\partial n} = c_2 & \text{on } \Gamma_N, \end{cases} \tag{13}$$

with $\mu \in \mathbb{R}^+$; $\Omega \subset \mathbb{R}^2$ is a regular bounded domain; $\sigma \in L^\infty(\Omega)$ with $\sigma \geq 0$ a.e. in Ω, $\mathbf{b} \in [L^\infty(\Omega)]^2$ with $\nabla \cdot \mathbf{b} \in L^\infty(\Omega)$ such that $-\frac{1}{2}\nabla \cdot \mathbf{b} + \sigma \geq 0$ a.e. in Ω and $\mathbf{b} \cdot \mathbf{n} \geq 0$ on Γ_N, $c_1 \in H^{1/2}(\Gamma_D)$, $c_2 \in L^2(\Gamma_N)$ and $f \in L^2(\Omega)$ are given functions; $\partial u/\partial n = \nabla u \cdot \mathbf{n}$ is the normal derivative of u, $\mathbf{n}$ being the unit outward normal vector to the boundary $\partial\Omega$ of the domain.
Here and throughout the paper we use a standard notation to denote both the Lebesgue and the Sobolev spaces of functions and the corresponding norms ([29]). The regularity demanded above for the data ensures the well-posedness of the weak formulation of (13).
In Sections 2.2.1 and 2.2.2 we particularize the model analysis above for two different choices of the bilinear forms $a(\cdot,\cdot)$ and $d(\cdot,\cdot)$ in (1). In both cases the goal functional J_{goal} is identified by the general representation

$$J_{goal}(v) = \int_{\omega} j_\omega \, v \, d\omega + \int_{\Gamma} j_\gamma \, v \, ds, \tag{14}$$

where $\omega \subseteq \Omega$, $\Gamma \subseteq \Gamma_N$, while $j_\omega \in L^2(\Omega)$ and $j_\gamma \in L^2(\Gamma)$ are suitable density functions.

2.2.1 ADR versus AD

As first example we swap between (13) and the advection-diffusion (AD) problem obtained by omitting the term σu in (13). The corresponding adapted primal problem is thus identified by (2) by letting

$$a(u_\alpha, w) = \int_\Omega \mu \nabla u_\alpha \cdot \nabla w \, d\Omega + \int_\Omega (\mathbf{b} \cdot \nabla u_\alpha) w \, d\Omega, \quad d(u_\alpha, \alpha w) = \int_\Omega \alpha \sigma u_\alpha w \, d\Omega,$$
$$F(w) = \int_\Omega f w \, d\Omega + \int_{\Gamma_N} c_2 w \, ds,$$

the function spaces being $V = W = H^1(\Omega)$, $V_0 = W_0 = H^1_{\Gamma_D}(\Omega)$.
According to (12) the model error estimator is now

$$\eta_\alpha = -d(u_\alpha, (1-\alpha)\,\widetilde{z}_\alpha) = -\int_\Omega (1-\alpha)\sigma u_\alpha \widetilde{z}_\alpha \, d\Omega, \tag{15}$$

$\widetilde{z}_\alpha$ being the weak solution to the dual problem

$$\begin{cases} -\mu\Delta\widetilde{z}_\alpha - \nabla \cdot (\mathbf{b}\widetilde{z}_\alpha) + \alpha\sigma\widetilde{z}_\alpha = j_\omega & \text{in } \Omega, \\ \widetilde{z}_\alpha = 0 & \text{on } \Gamma_D, \\ (\mu\nabla\widetilde{z}_\alpha + \mathbf{b}\widetilde{z}_\alpha) \cdot \mathbf{n} = j_\gamma & \text{on } \Gamma, \\ (\mu\nabla\widetilde{z}_\alpha + \mathbf{b}\widetilde{z}_\alpha) \cdot \mathbf{n} = 0 & \text{on } \Gamma_N \backslash \Gamma. \end{cases} \tag{16}$$

To exemplify the α-`adaptive procedure` associated with the estimator (15), we consider the following data: $\mu = 10^{-3}$, $\mathbf{b} = (x_2, -x_1)^T$, $\sigma = 0.5$, $f = 0$

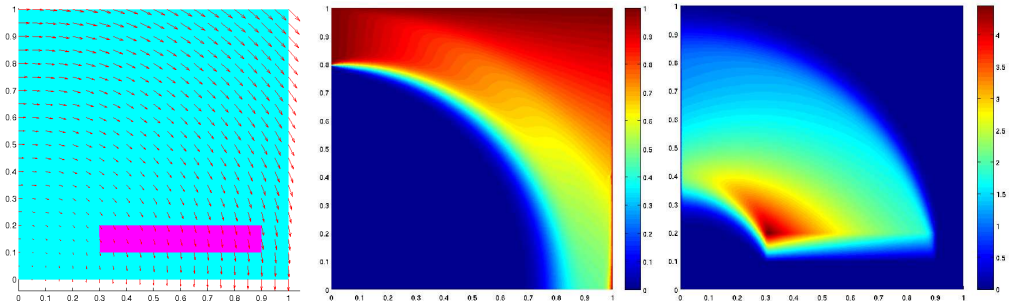

Figure 1: ADR vs AD (model adaptation): domain, advective field and target region (left), fine primal (middle) and dual (right) solutions.

and $\Omega = (0,1)^2$ (see Fig. 1 (left)). Concerning the boundary data, we assign a homogeneous Neumann condition on $\Gamma_N = \{(x_1, x_2) : x_2 = 0\}$, i.e., $c_2 = 0$ in (13); a homogeneous Dirichlet condition on $\{(0, x_2) : 0 < x_2 < 0.8\}$ and $u = 1$ elsewhere. The corresponding fine solution is displayed in Figure 1 (center). The functional J_{goal} coincides with the mean value of the solution on the area $E = (0.3, 0.9) \times (0.1, 0.2)$ (see Fig. 1 (left)), i.e.,

$$J_{goal}(v) = \frac{1}{|E|} \int_E v \, dE,$$

$|\omega|$ denoting the measure of the general set $\omega \subset \mathbb{R}^2$. This choice implies $j_\omega = |\omega|^{-1}$, with $\omega = E$, and $j_\gamma = 0$ in (14), i.e., in (16). We refer to Figure 1 (right) where the fine dual solution is shown. Finally, the value $\tau_m = 10^{-2}$ is selected for the tolerance in the α-`adaptive procedure`.
Figure 2 gathers the main steps of such a procedure which terminates after 5 iterations. In the first column we find the distribution of the areas Ω_1 (dark) and Ω_0 (light), in correspondence with the second, third and fifth iterations. The middle column collects the adapted primal solution computed on the areas distribution on the left. The last column furnishes the elementwise distribution of η_α evaluated on the adapted solutions in the center and on the corresponding dual variables.
The areas of influence detected by η_α are confined to the regions most meaningful for the goal functional, that is the ones around the circular internal layer of u_1 but upwind the observation region E. This is justified also by the behaviour of the dual solution in Figure 1 (right).
The percentage of the fine region Ω_1, at the last iteration, is only the 30% of $|\Omega|$. A comparison between the fine primal solution in Figure 1 (center) and the fifth adapted primal solution in Figure 2 (bottom-center) highlights the absence of the reaction contribution in the upper-right part of Ω.
Concerning the distribution of the error estimator, we observe that, during the adaptive procedure, its value decreases where the fine model is switched on until, at the last iteration, only a thin shell outside Ω_1 is somehow still meaningful.

A more quantitative analysis is provided in Table 1, where the percentage of the fine area, the estimator of the relative error, the actual relative error, and the model effectivity index E.I. $= \eta_\alpha / |J_{goal}(u_1) - J_{goal}(u_\alpha)|$ are summarized throughout all the five iterations. The fine areas cover a larger and larger portion

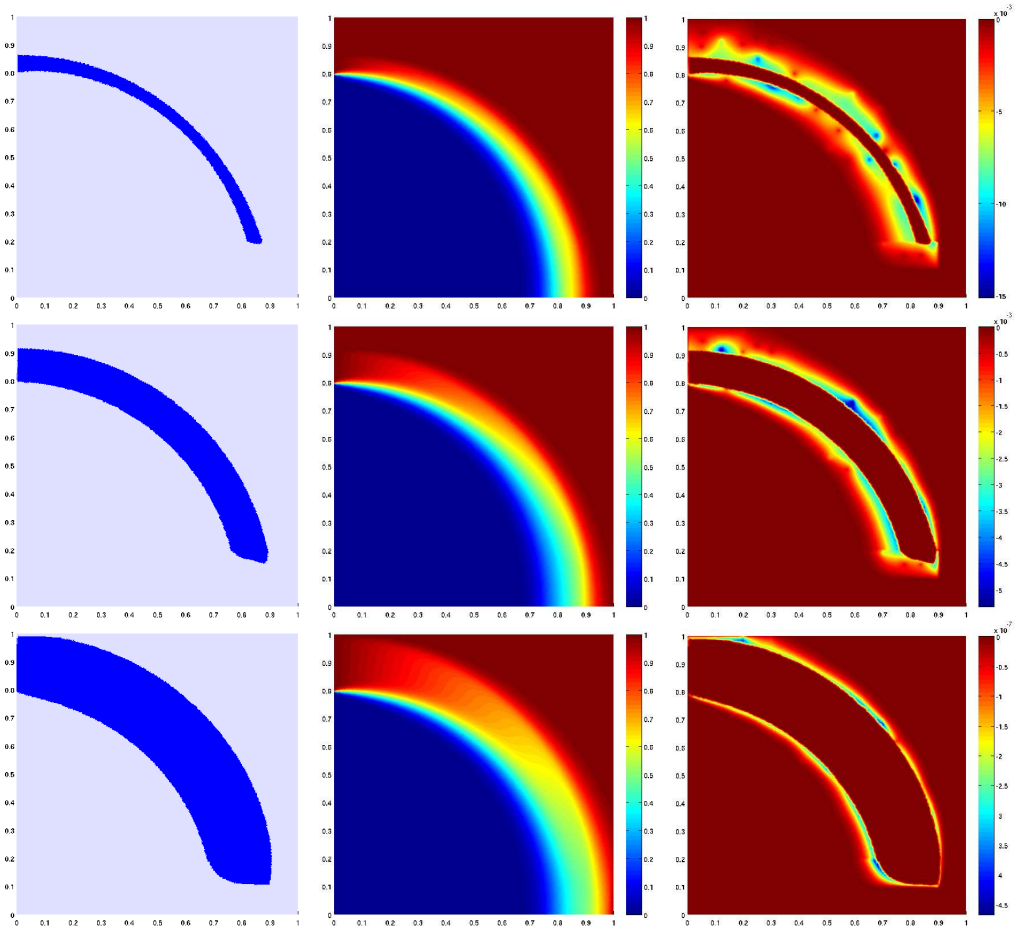

Figure 2: ADR vs AD (model adaptation): distribution of the areas Ω_1 and Ω_0 (left column), adapted primal solution (middle column) and elementwise distribution of η_α (right column) at the second (first row), third (second row) and fifth (third row) iteration.

up to about one third of the whole domain, while both the estimator and the error decrease steadily. The values of E.I., always close to 1, assess the robustness of the estimator η_α in (15).

2.2.2 ADR versus DR

As a second instance we alternate the ADR model with the diffusion-reaction problem (DR) obtained by dropping in (13) the advective term.
We recover the adapted formulation (2) by picking the function spaces as in

# it	$\lvert\Omega_1\rvert\%$	$\frac{\lvert\eta_\alpha\rvert}{\lvert J_{goal}(u_1)\rvert}$	$\frac{\lvert J_{goal}(u_1)-J_{goal}(u_\alpha)\rvert}{\lvert J_{goal}(u_1)\rvert}$	E.I.
1	0.00	$1.39 \cdot 10^{+00}$	$1.00 \cdot 10^{+00}$	1.39
2	5.00	$8.02 \cdot 10^{-01}$	$6.18 \cdot 10^{-01}$	1.30
3	15.00	$2.28 \cdot 10^{-01}$	$1.87 \cdot 10^{-01}$	1.22
4	25.00	$3.72 \cdot 10^{-02}$	$3.21 \cdot 10^{-02}$	1.16
5	30.00	$9.58 \cdot 10^{-03}$	$8.47 \cdot 10^{-03}$	1.13

Table 1: ADR vs AD (model adaptation): iteration, percentage of fine areas, estimator of the relative error, actual relative error, model effectivity index.

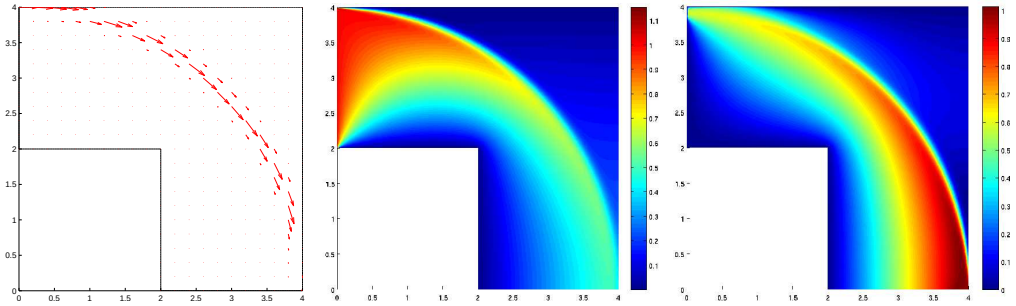

Figure 3: ADR vs DR (model adaptation): domain and advective field (left), fine primal (middle) and dual (right) solutions.

Section 2.2.1 and taking

$$a(u_\alpha, w) = \int_\Omega \mu \nabla u_\alpha \cdot \nabla w \, d\Omega + \int_\Omega \sigma u_\alpha w \, d\Omega, \quad d(u_\alpha, \alpha w) = \int_\Omega \alpha(\mathbf{b} \cdot \nabla u_\alpha) w \, d\Omega,$$
$$F(w) = \int_\Omega f w \, d\Omega + \int_{\Gamma_N} c_2 w \, ds.$$

The model error estimator (12) is thus

$$\eta_\alpha = -d(u_\alpha, (1-\alpha)\widetilde{z}_\alpha) = -\int_\Omega (1-\alpha)(\mathbf{b} \cdot \nabla u_\alpha)\widetilde{z}_\alpha \, d\Omega, \tag{17}$$

where $\widetilde{z}_\alpha$ is the weak solution to the dual problem

$$\begin{cases} -\mu\Delta\widetilde{z}_\alpha - \nabla \cdot (\alpha \mathbf{b}\widetilde{z}_\alpha) + \sigma\widetilde{z}_\alpha = j_\omega & \text{in } \Omega, \\ \widetilde{z}_\alpha = 0 & \text{on } \Gamma_D, \\ (\mu\nabla\widetilde{z}_\alpha + \alpha\mathbf{b}\widetilde{z}_\alpha) \cdot \mathbf{n} = j_\gamma & \text{on } \Gamma, \\ (\mu\nabla\widetilde{z}_\alpha + \alpha\mathbf{b}\widetilde{z}_\alpha) \cdot \mathbf{n} = 0 & \text{on } \Gamma_N \backslash \Gamma. \end{cases}$$

To assess the performance of the estimator (17), we pick the L-shaped domain in Figure 3 (left). The physical parameters are chosen as: $\mu = 10^{-3}$; $\sigma = 10^{-4}$; $\mathbf{b} = (V\sin(\theta), -V\cos(\theta))^T$, where $\theta = \arctan(x_2/x_1)$, $V = \exp(-(r-4)^2/0.01)$ and

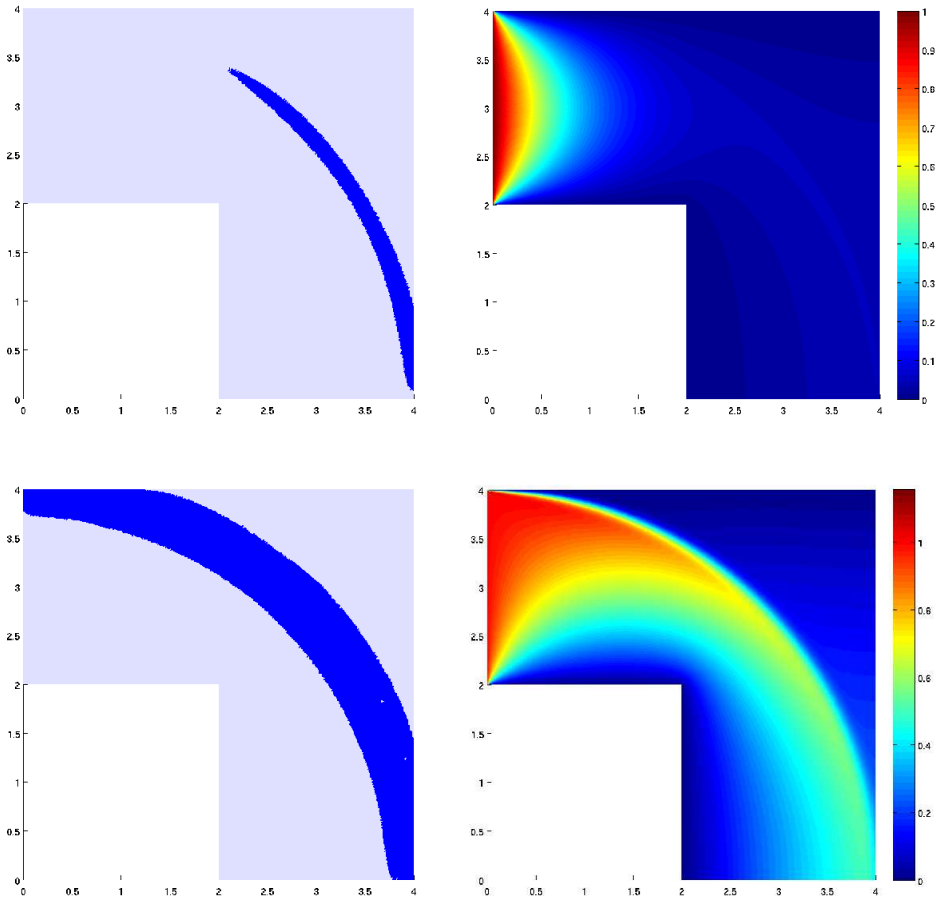

Figure 4: ADR vs DR (model adaptation): distribution of the areas Ω_1 and Ω_0 (left column) and adapted primal solution (right column) at the second (top row) and last (bottom row) iteration.

$r = \sqrt{x_1^2 + x_2^2}$ (see Fig. 3 (left)); $f = 0$. We enforce a homogeneous Neumann condition ($c_2 = 0$) along $\Gamma_N = \{(4, x_2) : 0 < x_2 < 4\} \cup \{(x_1, 0) : 2 < x_1 < 4\}$; the nonhomogeneous Dirichlet condition $u = 1$ on the edge $\{(0, x_2) : 2 < x_2 < 4\}$, while $u = 0$ elsewhere.

The choice made for the data leads to a fine solution u_1 characterized by a thin circular internal layer around $r = 4$ (see Fig. 3 (middle)). The functional J_{goal} is now related to a boundary observation, i.e., to the convective flux

$$J_{goal}(v) = \int_\Gamma \mathbf{b} \cdot \mathbf{n}\, v\, ds,$$

with $\Gamma = \{(x_1, 0) : 2 < x_1 < 4\}$.

For a global model tolerance $\tau_m = 10^{-2}$, the α-`adaptive procedure` yields four iterations. The fine/coarse area distribution and the corresponding adapted primal solution at the second and last iteration are provided in Figure 4. It can be noticed that, at the second iteration, the area where the advective contribution is solved is very small, and consequently the corresponding adapted solution exhibits a predominant diffusive behaviour (Fig. 4 (top)). On the contrary, at the last iteration, the advective term is switched on in a meaningful zone

embracing the internal layer (Fig. 4 (bottom-left)). This identifies an adapted solution where the convective features are evident (see Fig. 4 (bottom-right)). As expected, the dominant advective character of the problem at hand, associated with an outflow boundary observation area, lead the estimator η_α to identify the regions most sensitive to the field $\mathbf{b}$.

The same quantities as in Table 1 are computed also for this test case (see Table 2). At the last iteration, the fine model is solved on only one fourth of Ω. Both the relative estimator and error decrease throughout the iterations. The effectivity index, just at the fourth iteration reaches a value corroborating the robustness of the estimator (17). Notice the large overestimation by η_α at the first iteration due to the complete neglecting of the advection, crucial to control the boundary flux.

# it	$\lvert\Omega_1\rvert\%$	$\frac{\lvert\eta_\alpha\rvert}{\lvert J_{goal}(u_1)\rvert}$	$\frac{\lvert J_{goal}(u_1)-J_{goal}(u_\alpha)\rvert}{\lvert J_{goal}(u_1)\rvert}$	E.I.
1	0.00	$1.71 \cdot 10^{+02}$	$1.01 \cdot 10^{+00}$	169.81
2	5.00	$1.16 \cdot 10^{+02}$	$1.39 \cdot 10^{+00}$	83.29
3	15.00	$7.64 \cdot 10^{+00}$	$4.44 \cdot 10^{-01}$	17.20
4	25.00	$3.32 \cdot 10^{-03}$	$1.25 \cdot 10^{-03}$	2.66

Table 2: ADR vs DR (model adaptation): iteration, percentage of fine areas, estimator of the relative error, actual relative error, model effectivity index.

3 An a posteriori model analysis: the nonlinear case

With a view to the modelization of real-life phenomena, it is unavoidable to deal with nonlinear problems. Nonetheless the corresponding analysis is no doubt more cumbersome. The standard mathematical approach used to handle a goal-oriented analysis in a nonlinear framework is based on a reformulation of the problem at hand as a constrained minimization problem, hinging on a suitable Lagrangian functional. In general the most critical issues to be tackled in the definition of the Lagrangian are the treatment of the nonhomogeneous Dirichlet boundary data as well as the inclusion of possible stabilization terms in the discrete variational formulation.
Concerning the extension of the model error analysis in Section 2 to the nonlinear case, the approach that manages nonhomogeneous conditions via suitable affine function spaces can still be pursued. This would entail a generalization of the analysis in [9, 26, 33] to the model setting. However, the later merging of the model with the discretization analysis suggests undertaking a simpler approach, based on the weak imposition of the nonhomogeneous Dirichlet conditions (see, e.g., [14, 3]).

Let us consider the general weak formulation of the differential problem at hand:

$$\text{find } u_1 \in V: \quad a(u_1)(w) + d(u_1)(w) = F(w) \quad \forall w \in W, \tag{18}$$

where $a(\cdot)(\cdot)$ and $d(\cdot)(\cdot)$ are semilinear forms, i.e. linear with respect to the second argument and nonlinear in the first one. Analogously to the linear case $a(\cdot)(\cdot)$ identifies the coarse model, whereas $d(\cdot)(\cdot)$ represents the correction leading to the fine model. Assumptions similar to the ones advanced on $d(\cdot,\cdot)$ in

Section 2 are demanded also in this case. We point out that (18) is still a Petrov-Galerkin formulation. Moreover the forms $a(\cdot)(\cdot)$ and $F(\cdot)$ suitably take into account the nonhomogeneous Dirichlet boundary conditions, thus weakly enforced.
Let us then introduce the adapted problem depending on α:

$$\text{find } u_\alpha \in V: \quad a(u_\alpha)(w) + d(u_\alpha)(\alpha w) = F(w) \quad \forall w \in W, \tag{19}$$

α being defined as in the previous section.

Let $J_{goal} : V \to \mathbb{R}$ be the target functional of interest, now possibly nonlinear. We aim at finding a computable error estimator η_α of the output model error $J_{goal}(u_1) - J_{goal}(u_\alpha)$. For this purpose, we introduce the following (trivial) constrained minimization problem ([9]), after assuming the existence and the uniqueness of the solution u_α to (19) in V:

$$\text{find } u_\alpha \in V: \quad \inf_{v \in M_\alpha} J_{goal}(v) = J_{goal}(u_\alpha), \tag{20}$$

where $M_\alpha = \{v \in V: \ a(v)(\xi) + d(v)(\alpha\xi) = F(\xi), \forall \xi \in W\}$. This formulation allows us to resort to the standard Lagrangian theory to enforce the constraint. We introduce the adapted Lagrangian $\mathcal{L}_\alpha : V \times W \to \mathbb{R}$

$$\mathcal{L}_\alpha(u_\alpha, z_\alpha) = J_{goal}(u_\alpha) + F(z_\alpha) - a(u_\alpha)(z_\alpha) - d(u_\alpha)(\alpha z_\alpha), \tag{21}$$

z_α being the Lagrange multiplier associated with the constraint in M_α.
The solution to (20) is equivalent to finding the saddle-point of (21), such that

$$\mathcal{L}'_\alpha(u_\alpha, z_\alpha)(\psi, \phi) = 0 \quad \forall (\psi, \phi) \in V \times W.$$

We are consequently led to solve problem (19) together with the *dual adapted* problem

$$\text{find } z_\alpha \in W: \quad a'(u_\alpha)(z_\alpha, \psi) + d'(u_\alpha)(\alpha z_\alpha, \psi) = J'_{goal}(u_\alpha)(\psi) \quad \forall \psi \in V, \tag{22}$$

where $a'(u_\alpha)(\cdot, \psi)$ and $d'(u_\alpha)(\cdot, \psi)$ denote the Fréchet derivatives of $a(u_\alpha)(\cdot)$ and $d(u_\alpha)(\cdot)$, respectively, with respect to u_α and evaluated at ψ.
With a view to the desired estimator η_α, the Lagrangian $\mathcal{L}_1$ associated with the fine problem can be related to the adapted one $\mathcal{L}_\alpha$ via relation

$$\mathcal{L}_1(u, z) = \mathcal{L}_\alpha(u, z) - d(u)((1-\alpha)z), \quad \forall (u, z) \in V \times W.$$

Let us introduce the primal $\rho(u_\alpha)(\cdot) : W \to \mathbb{R}$ and the dual $\rho^*(u_\alpha)(z_\alpha, \cdot) : V \to \mathbb{R}$ *model residuals* given by

$$\begin{aligned}
&\rho(u_\alpha)(\cdot) = F(\cdot) - a(u_\alpha)(\cdot) - d(u_\alpha)(\cdot), \\
&\rho^*(u_\alpha)(z_\alpha, \cdot) = J'_{goal}(u_\alpha)(\cdot) - a'(u_\alpha)(z_\alpha, \cdot) - d'(u_\alpha)(z_\alpha, \cdot).
\end{aligned}$$

By mimicking the proof of Lemma 2.3, we obtain the identities

$$\rho(u_\alpha)(\cdot) = -d(u_\alpha)((1-\alpha)\cdot), \quad \rho^*(u_\alpha)(z_\alpha, \cdot) = -d'(u_\alpha)((1-\alpha)z_\alpha, \cdot).$$

We are in a position to state the a posteriori model output error control:

Proposition 3.1 *For $a(\cdot)(\cdot)$, $d(\cdot)(\cdot)$ and $J_{goal}(\cdot)$ smooth enough, we have*

$$J_{goal}(u_1) - J_{goal}(u_\alpha) = -d(u_\alpha)((1-\alpha)z_\alpha) + \frac{1}{2}\Big[\rho(u_\alpha)(e_z) + \rho^*(u_\alpha)(z_\alpha, e_u)\Big] + R, \tag{23}$$

where $e_u = u_1 - u_\alpha$ and $e_z = z_1 - z_\alpha$ are the primal and dual model error, respectively, while

$$R = \frac{1}{2}\int_0^1 \mathcal{L}_1'''(u_\alpha + se_u, z_\alpha + se_z)(\{e_u, e_z\}, \{e_u, e_z\}, \{e_u, e_z\})s(s-1)ds,$$

is the remainder, with z_1 the fine dual solution to (22) for α identically equal to 1.

Proof. We refer to the appendix in [43]. □

We stress that relation (23) provides us with an exact representation of the model error $J_{goal}(u_1) - J_{goal}(u_\alpha)$ though not explicitly computable as depending on the fine solutions u_1 and z_1. Thus we adopt as model error estimator η_α the only computable term in (23), namely

$$\eta_\alpha = -d(u_\alpha)((1-\alpha)z_\alpha) \ \big(\equiv \rho(u_\alpha)(z_\alpha)\big). \tag{24}$$

In [10] some theoretical assumptions are supplied to justify the dropping of the two residuals $\rho(u_\alpha)(e_z)$ and $\rho^*(u_\alpha)(z_\alpha, e_u)$ and of the remainder R in (23), while in [43] these hypotheses are numerically corroborated in the unsteady shallow water setting.

Remark 3.1 *On comparing the definitions of the model estimators in (12) and (24), we see that the two estimators coincide formally. Indeed, the dual solution z_α to (22) can be shown to satisfy homogeneous Dirichlet boundary conditions (see, e.g., [31]), analogously to $\widetilde{z}_\alpha$ in the linear case.*

3.1 Some examples

The model estimator for the nonlinear case is assessed on two 2D test cases, scalar and vector, respectively. The corresponding model adaptive procedure coincides exactly with the one in Section 2.1.

3.1.1 A scalar problem: a logistic population model

As an instance of nonlinear scalar problem we consider the logistic population model typical of population dynamics (see, e.g., [35, 36]). We are interested in the study of diffusion mechanisms, modeling the movement of many individuals in an environment or media. The individuals can be very tiny (e.g., bacteria, molecules, cells) or large objects (e.g., animals, plants). In particular we deal with the stationary case by assuming that the spatial distribution of the individual density u at hand has reached the steady state. The reference model is

$$\begin{cases} -\mu\Delta u + \mathbf{b}\cdot\nabla u - \sigma u + \gamma u^2 = f & \text{in } \Omega, \\ u = 0 & \text{on } \Gamma_D, \\ \mu\dfrac{\partial u}{\partial n} = c_2 & \text{on } \Gamma_N, \end{cases} \tag{25}$$

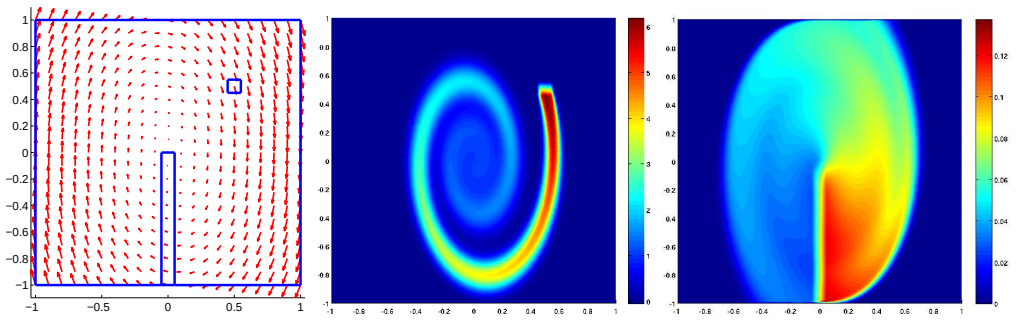

Figure 5: Logistic population (model adaptation): domain, advective field and target region (left), fine primal (middle) and dual (right) solutions.

with $\sigma, \gamma > 0$ a.e. in Ω, and where all the other data satisfy the same regularity assumptions as in Section 2.2. However, to guarantee the well-posedness of the weak form associated with (25) some further conditions have to be demanded on the data.
The positiveness of σ and γ instills the logistic growth feature to the considered population, since the global reactive term $-\sigma u + \gamma u^2$ in $(25)_1$ can be rewritten in the standard form $-\sigma u\,(1 - \gamma/\sigma u)$, with σ the linear reproduction rate and σ/γ the carrying capacity of the environment ([35, 36]).
The diffusive term in (25) models the random dispersion of the species, the advective term takes into account some possible transport phenomenon while f describes an external injection or withdrawal. Concerning the assigned boundary conditions, the boundary Γ_D mimics a hostile portion of the borders while the Neumann datum specifies an immigration or emigration flux.
We refer to [42] and [47] for a theoretical investigation about variants of model (25).

We employ here the logistic model (25) for describing the motion of a school of fishes in a small area off sea. This is reasonable under the assumption that the vertical motion of the fishes is negligible and that the portion of the sea is sufficiently large compared to the dimension of the fishes. In particular, the domain Ω coincides with the square $(-1, 1)^2$. The other data are $\mu = 10^{-3}$, $\mathbf{b} = (x_2 - 0.1x_1, 3(-x_1 - 0.1x_2))^T$, with $\nabla \cdot \mathbf{b} = -0.4$, $\sigma = 10^{-2}$, $\gamma = 2 \times 10^{-2}$, $f = 100\chi_E$, with $E = (0.45, 0.55) \times (0.45, 0.55)$ (see Fig. 5 (left)). Full homogeneous Dirichlet boundary conditions are assigned on $\partial\Omega$. The fine primal solution is heavily dominated by the spiral shaped field $\mathbf{b}$, as evident in Figure 5 (center). The damping of the solution towards the center of the domain is due to both the negative divergence of $\mathbf{b}$ and to the logistic term.

As we are interested in measuring the fish flux across a rectangular creel $C_r = (-0.05, 0.05) \times (-1, 0)$ (see Fig. 5 (left)), we identify the functional J_{goal} as

$$J_{goal}(v) = -\int_{C_r} b_1 v \, dC_r,$$

where b_1 is the first component of $\mathbf{b}$.

With reference to the model adaptation framework, (25) identifies the fine problem. On the other hand to define the coarse problem we give up the computationally most expensive term, that is the nonlinear contribution γu^2. This

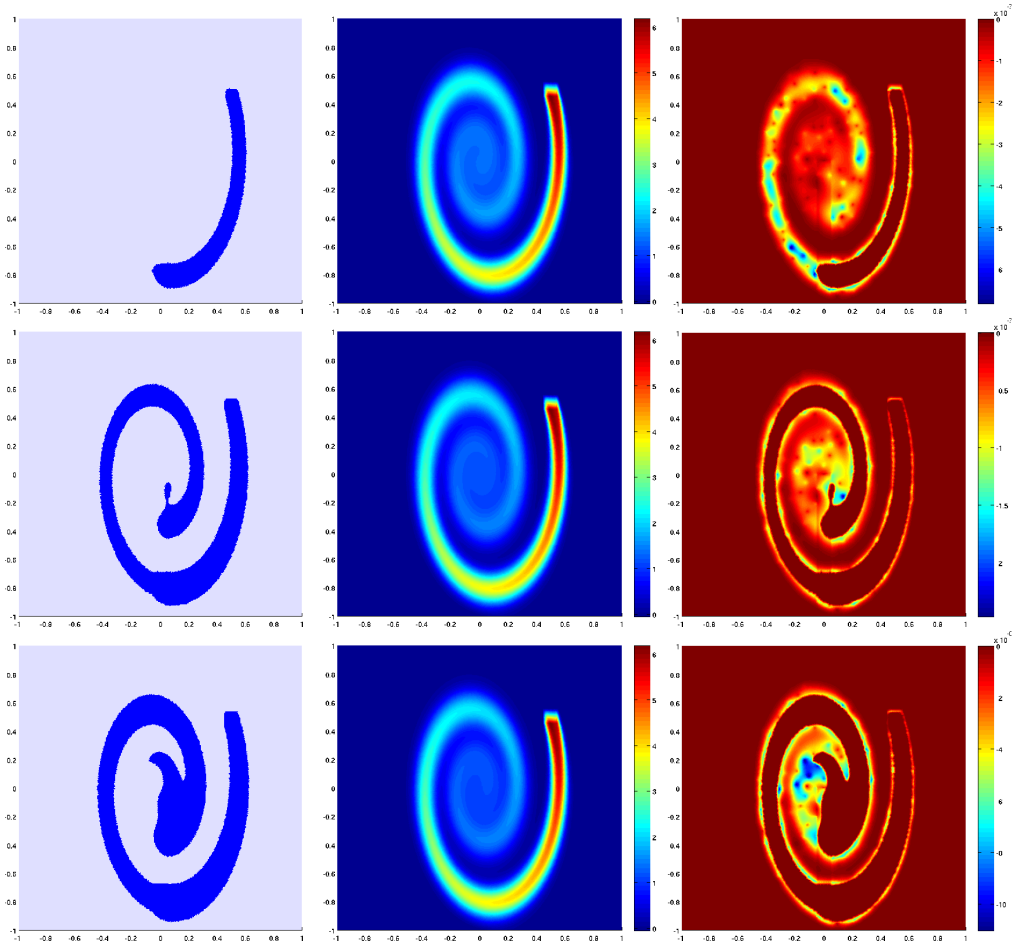

Figure 6: Logistic population (model adaptation): distribution of the areas Ω_1 and Ω_0 (left column), adapted primal solution (middle column) and elementwise distribution of η_α (right column) at the second (first row), third (second row) and fourth (third row) iteration.

amounts to allowing for a simple Malthusian growth ([35, 36]). Consequently the adapted primal problem turns out to be

$$\begin{cases} -\mu\Delta u_\alpha + \mathbf{b}\cdot\nabla u_\alpha - \sigma u_\alpha + \alpha\gamma u_\alpha^2 = f & \text{in } \Omega, \\ u_\alpha = 0 & \text{on } \Gamma_D, \\ \mu\dfrac{\partial u_\alpha}{\partial n} = c_2 & \text{on } \Gamma_N, \end{cases} \tag{26}$$

whose weak form coincides with (19), where $V = W = H^1(\Omega)$, and where the

# it	$\lvert\Omega_1\rvert\%$	$\frac{\lvert\eta_\alpha\rvert}{\lvert J_{goal}(u_1)\rvert}$	$\frac{\lvert J_{goal}(u_1)-J_{goal}(u_\alpha)\rvert}{\lvert J_{goal}(u_1)\rvert}$	E.I.
1	0.00	$1.49 \cdot 10^{-01}$	$1.28 \cdot 10^{-01}$	1.17
2	5.51	$4.51 \cdot 10^{-02}$	$3.90 \cdot 10^{-02}$	1.16
3	16.52	$1.19 \cdot 10^{-02}$	$1.10 \cdot 10^{-02}$	1.08
4	21.63	$5.60 \cdot 10^{-03}$	$5.35 \cdot 10^{-03}$	1.05

Table 3: Logistic population (model adaptation): iteration, percentage of fine areas, estimator of the relative error, actual relative error, model effectivity index.

forms $a(\cdot)(\cdot)$, $d(\cdot)(\cdot)$ and $F(\cdot)$ are defined by

$$\begin{aligned} a(u_\alpha)(w) &= \int_\Omega \mu \nabla u_\alpha \cdot \nabla w \, d\Omega + \int_\Omega (\mathbf{b} \cdot \nabla u_\alpha) w \, d\Omega - \int_\Omega \sigma u_\alpha w \, d\Omega + \lambda \int_{\Gamma_D} u_\alpha w \, ds, \\ d(u_\alpha)(\alpha\, w) &= \int_\Omega \alpha\gamma u_\alpha^2 w \, d\Omega, \quad F(w) = \int_\Omega f w \, d\Omega + \int_{\Gamma_N} c_2 w \, ds, \end{aligned} \tag{27}$$

with λ a suitable penalty parameter used to impose weakly the Dirichlet datum. Thus, according to the general recipe (24), the model error estimator for the logistic population model (25) is

$$\eta_\alpha = -d(u_\alpha)((1-\alpha)\, z_\alpha) = -\int_\Omega (1-\alpha)\gamma u_\alpha^2 z_\alpha \, d\Omega, \tag{28}$$

z_α being the solution to the adapted dual problem

$$\begin{cases} -\mu\Delta z_\alpha - \nabla \cdot (\mathbf{b} z_\alpha) - \sigma z_\alpha + 2\alpha\gamma u_\alpha z_\alpha = -b_1 \chi_{C_r} & \text{in } \Omega, \\ z_\alpha = 0 & \text{on } \Gamma_D, \\ (\mu \nabla z_\alpha + \mathbf{b} z_\alpha) \cdot \mathbf{n} = 0 & \text{on } \Gamma_N. \end{cases}$$

We remark the linearity of the adapted dual problem leading to a corresponding Malthusian growth provided by the linear reproduction rate $\sigma - 2\alpha\gamma u_\alpha$.

The α-`adaptive procedure` is run with a global tolerance $\tau_m = 10^{-2}$ and stops after 4 iterations. Figure 6 collects the distribution of the fine and coarse areas (first column), the corresponding adapted primal solution (middle column) and the elementwise distribution of the estimator in (24) at the second (first row), third (second row), and fourth (third row) iteration. The fine regions gradually crowd around the streamlines stemming from the release area E. We point out that also a portion of the central region of Ω contributes to the fine model, as shown by the transition from the third to the fourth iteration, though to a lesser extent as in the meantime the density of the fishes moving inward has decreased. The distribution of η_α keeps up with this gradual updating of the fine regions and takes on a maximum absolute value of about 10^{-7} on the last adapted model. No macroscopic difference can be appreciated on comparing the three adapted primal solutions in Figure 6.

The good performance of both the error estimator in (24) and the α-`adaptive procedure` are confirmed by the values reported in Table 3.

3.1.2 A vector problem: a predator-prey system

Different species interact in ecological problems (foxes and rabbits, lions and gazelles, etc) as well as different substances react and produce new compounds in chemical reactions. In all these events systems of differential equations are used to model the phenomena (e.g., predator-prey, Gierer-Meinhordt, Gray-Scott models, see [35, 36]). In the following we analyze system

$$\begin{cases} -\mu_u \Delta u + \mathbf{b} \cdot \nabla u - \sigma_u u + \gamma u v = f_u & \text{in } \Omega, \\ -\mu_v \Delta v + \mathbf{b} \cdot \nabla v + \sigma_v v - K \gamma u v = f_v & \text{in } \Omega, \\ u = h_u & \text{on } \Gamma_D, \\ v = h_v & \text{on } \Gamma_D, \\ \mu_u \dfrac{\partial u}{\partial n} = g_u & \text{on } \Gamma_N, \\ \mu_v \dfrac{\partial v}{\partial n} = g_v & \text{on } \Gamma_N, \end{cases} \tag{29}$$

i.e., a variant of the standard Lotka-Volterra predator-prey model, enriched with convective and source terms. As in the previous section we are still interested in the steady solution. In particular, u and v stand for the prey and the predator density, respectively; the coefficients μ_u, $\mu_v \in \mathbb{R}^+$ are the corresponding species diffusion constants; $\sigma_u, \sigma_v, \gamma \in L^\infty(\Omega)$ are positive functions a.e. in Ω and represent the prey growth rate, the predator death rate and the death rate per encounter of preys due to predation, respectively; the constant K measures the efficiency of turning the preys into predators; $f_u, f_v \in L^2(\Omega)$ model possible sources external to the system at hand; $\mathbf{b} \in [L^\infty(\Omega)]^2$, with $\nabla \cdot \mathbf{b} \in L^\infty(\Omega)$, introduces an advection (for instance, a flow in a chemical reactor); Γ_D is the portion of the ecological system border where Dirichlet data (h_u and h_v) are assigned, while $g_u, g_v \in L^2(\Gamma_N)$ describe inward/outward random walks of the two species. All these parameters are tuned so that a unique (weak) solution to (29) is guaranteed.

In more detail, we consider a square domain $\Omega = (0,1)^2$ where two species of interest are released. The first species (prey) is able to sustain itself with other natural resources, while the second is a species of predators and survives eating the prey. The concentration of the two populations takes on the values $u = 1$ and $v = 0$ on $\{(0, x_2) : 0.6 < x_2 < 0.65\} \cup \{(0, x_2) : 0.75 < x_2 < 0.8\}$, and $u = 0$ and $v = 0.1$ on $\{(0, x_2) : 0.65 < x_2 < 0.75\} \cup \{(1, x_2) : 0.7 < x_2 < 0.8\}$. Moreover homogeneous Neumann conditions are imposed on $\Gamma_N = \{(x_1, 0) : 0.4 < x_1 < 0.6\}$ while homogeneous Dirichlet conditions are assigned elsewhere. Both species move in the domain by a random diffusion motion ($\mu_u = \mu_v = 5 \times 10^{-4}$) and are drifted by the advective field $\mathbf{b}$ in Figure 7 (left), which represents the solution to the Navier-Stokes equations characterized by a Reynolds number $Re = 100$ and completed with the following boundary data: parabolic profiles with average value 0.02 and 0.01 are enforced at the inflow boundaries $\{(0, x_2) : 0.6 < x_2 < 0.8\}$ and $\{(1, x_2) : 0.7 < x_2 < 0.8\}$, respectively; a homogeneous Neumann condition is assigned at the outflow $\Gamma_N = \{(x_1, 0) : 0.4 < x_1 < 0.6\}$, while no slip conditions hold elsewhere.
Concerning the other data in (29), we have: $\sigma_u = 10^{-2}$, $\sigma_v = 10^{-1}$, $\gamma = 1$,

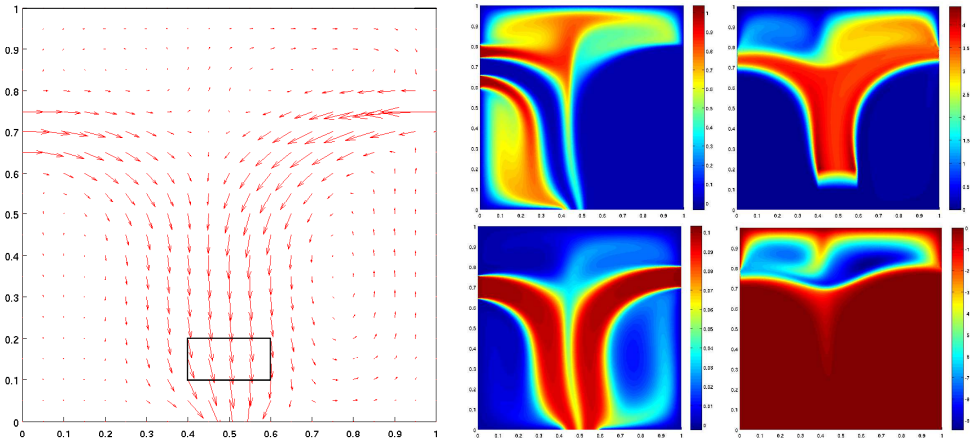

Figure 7: Predator-prey system (model adaptation): domain, advective field and observation area (left); fine primal solution (middle), u (top) and v (bottom); fine dual solution (right), $z_{\alpha,1}$ (top) and $z_{\alpha,2}$ (bottom).

$K = 0.1$, $f_u = 0$ and $f_v = 0$.
Figure 7 (middle) collects the fine solutions u and v to (29). Note the different distribution of the prey (top) and predator (bottom), strongly influenced by the boundary conditions and the field $\mathbf{b}$.

Our goal is to measure the average concentration of the preys in an area of interest $O_A = (0.4, 0.6) \times (0.1, 0.2)$ (see Fig. 7 (left)). This amounts to selecting as target functional

$$J_{goal}(u) = \frac{1}{|O_A|} \int_{O_A} u \, dO_A. \tag{30}$$

The corresponding dual solution is displayed in Figure 7 (right). Qualitatively, the first dual component seems to be the most relevant for influencing J_{goal}.

With a view to the model adaptation, both the nonlinear terms in (29) are switched on/off. The corresponding adapted system is thus

$$\begin{cases} -\mu_u \Delta u_\alpha + \mathbf{b} \cdot \nabla u_\alpha - \sigma_u u_\alpha + \alpha\gamma u_\alpha v_\alpha = f_u & \text{in } \Omega, \\ -\mu_v \Delta v_\alpha + \mathbf{b} \cdot \nabla v_\alpha + \sigma_v v_\alpha - \alpha K \gamma u_\alpha v_\alpha = f_v & \text{in } \Omega, \\ u_\alpha = h_u & \text{on } \Gamma_D, \\ v_\alpha = h_v & \text{on } \Gamma_D, \\ \mu_u \dfrac{\partial u_\alpha}{\partial n} = g_u & \text{on } \Gamma_N, \\ \mu_v \dfrac{\partial v_\alpha}{\partial n} = g_v & \text{on } \Gamma_N. \end{cases}$$

The vector feature of the problem at hand leads us to introduce a proper notation. Let $U = (u, v)$ and $U_\alpha = (u_\alpha, v_\alpha)$ be the pairs of fine and adapted primal solutions, respectively, both belonging to the space $V = W = [H^1(\Omega)^2]$. The weak form of the adapted primal problem is given by

$$\text{find } U_\alpha \in V : \;\; a(U_\alpha)(\mathbf{W}) + d(U_\alpha)(\alpha\, \mathbf{W}) = F(\mathbf{W}) \quad \forall \mathbf{W} = (w_1, w_2) \in W, \tag{31}$$

where

$$
\begin{aligned}
a(U_\alpha)(\mathbf{W}) \quad &= \int_\Omega \mu_u \nabla u_\alpha \cdot \nabla w_1 \, d\Omega + \int_\Omega (\mathbf{b} \cdot \nabla u_\alpha) w_1 \, d\Omega - \int_\Omega \sigma_u u_\alpha w_1 \, d\Omega \\
&\quad + \int_\Omega \mu_v \nabla v_\alpha \cdot \nabla w_2 \, d\Omega + \int_\Omega (\mathbf{b} \cdot \nabla v_\alpha) w_2 \, d\Omega + \int_\Omega \sigma_v v_\alpha w_2 \, d\Omega \\
&\quad + \lambda \int_{\Gamma_D} u_\alpha w_1 \, ds + \lambda \int_{\Gamma_D} v_\alpha w_2 \, ds, \\
d(U_\alpha)(\alpha\, \mathbf{W}) \quad &= \int_\Omega \alpha\gamma u_\alpha v_\alpha (w_1 - K w_2) \, d\Omega, \\
F(\mathbf{W}) \quad &= \int_\Omega (f_u w_1 + f_v w_2) \, d\Omega + \int_{\Gamma_N} (g_u w_1 + g_v w_2) \, ds + \lambda \int_{\Gamma_D} h_u w_1 \, ds \\
&\quad + \lambda \int_{\Gamma_D} h_v w_2 \, ds.
\end{aligned}
$$

The model error estimator for the predator-prey system (29) is thus

$$
\eta_\alpha = -d(U_\alpha)((1-\alpha)\, Z_\alpha) = -\int_\Omega (1-\alpha)\gamma u_\alpha v_\alpha (z_{\alpha,1} - K z_{\alpha,2}) \, d\Omega, \tag{32}
$$

$Z_\alpha = (z_{\alpha,1}, z_{\alpha,2})$ being the solution to the adapted dual problem

$$
\begin{cases}
-\mu_u \Delta z_{\alpha,1} - \nabla \cdot (\mathbf{b} z_{\alpha,1}) - \sigma_u z_{\alpha,1} + \alpha\gamma v_\alpha (z_{\alpha,1} - K z_{\alpha,2}) = \dfrac{1}{|O_A|} \chi_{O_A} & \text{in } \Omega, \\
-\mu_v \Delta z_{\alpha,2} - \nabla \cdot (\mathbf{b} z_{\alpha,2}) + \sigma_v z_{\alpha,2} + \alpha\gamma u_\alpha (z_{\alpha,1} - K z_{\alpha,2}) = 0 & \text{in } \Omega, \\
z_{\alpha,1} = z_{\alpha,2} = 0 & \text{on } \Gamma_D, \\
(\mu_u \nabla z_{\alpha,1} + \mathbf{b} z_{\alpha,1}) \cdot \mathbf{n} = 0 & \text{on } \Gamma_N, \\
(\mu_v \nabla z_{\alpha,2} + \mathbf{b} z_{\alpha,2}) \cdot \mathbf{n} = 0 & \text{on } \Gamma_N
\end{cases}
$$

associated with the functional in (30) and with the primal problem (31).
The α-`adaptive procedure` is tested on this configuration with a global tolerance $\tau_m = 10^{-2}$. The stopping criterion is met after 4 iterations.
Figure 8 shows the distribution of the regions Ω_1 and Ω_0 at the last three iterations. The zones firstly detected are those where the predator-prey interaction is stronger, i.e., where the "overlapping" between the predator and prey fluxes is meaningful. Successively, the influence of the dual solution and of the advective field leads to enrich the initial fine area with the contribution of the central and upper-right parts of the domain (compare Fig. 8 (right) with Fig. 7 (right)).
In Figure 9, we gather the prey (left) and predator (center) concentration at the first iteration, when the full coarse problem is approximated (top), and at the last α-`adaptive iteration` (bottom). For both species, the main difference can be appreciated in the top-right part of the domain. In the right column of Figure 9, the model estimator in (32) is plotted on each element $K \in \mathcal{T}_h$ at the first (top) and last (bottom) iteration. The values of η_α reduce considerably at the end of the model adaptive procedure, passing from an order

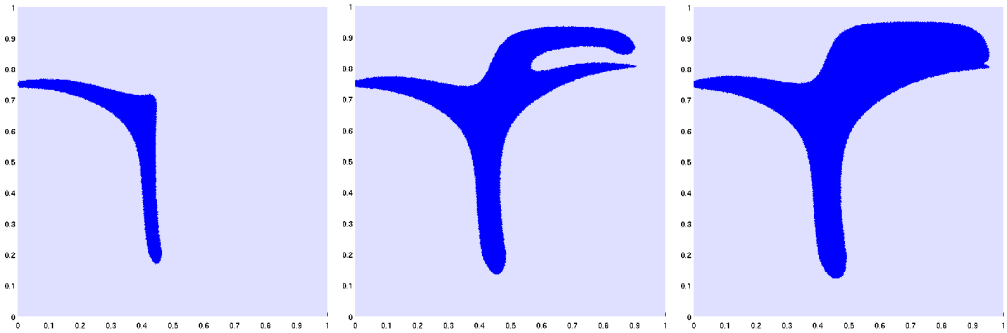

Figure 8: Predator-prey system (model adaptation): distribution of the fine and coarse areas at the second (left), third (middle) and fourth (right) iteration.

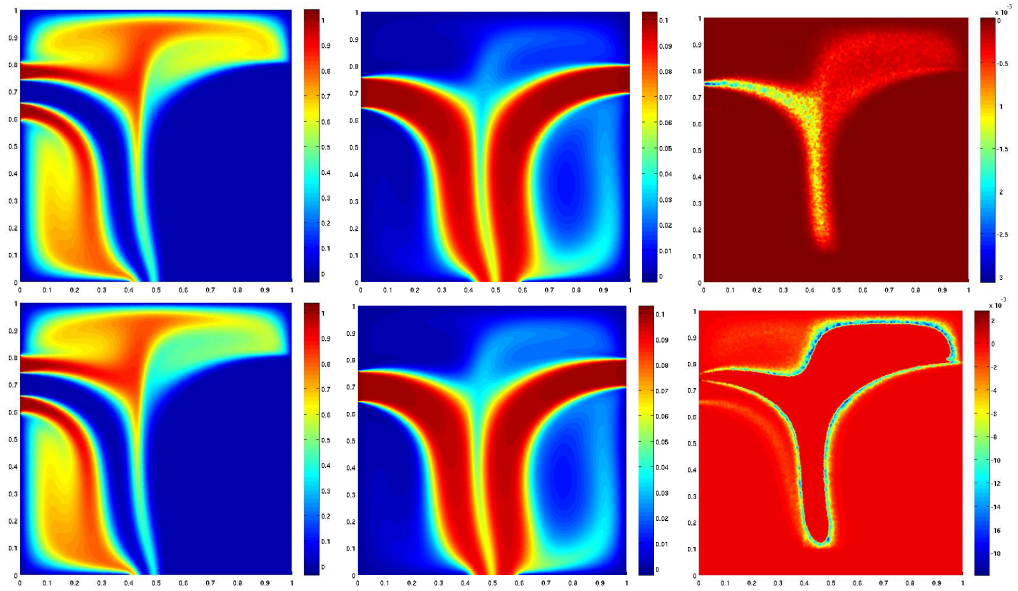

Figure 9: Predator-prey system (model adaptation): adapted prey (left) and predator (middle) density, and elementwise distribution of η_α at the first (top) and last (bottom) iteration.

of 10^{-6} down to 10^{-8}. Finally, Table 4 provides us with some quantitative information about the procedure in Section 2.1. At the final step, the final model is activated only on the 20% of Ω; both the quantities $|\eta_\alpha|/|J_{goal}(u_1)|$ and $|J_{goal}(u_1) - J_{goal}(u_\alpha)|/|J_{goal}(u_1)|$ decrease all along the iterations; the effectivity index confirm the good robustness of η_α, even though, in this case, it is slightly under estimating.

4 An anisotropic a posteriori analysis for the discretization error

We introduce the anisotropic setting used to enrich the model error analysis with directional information. In particular, in Section 4.1 we introduce the anisotropic framework, while in Section 4.2 a goal-oriented anisotropic error estimator is

# it	$\lvert\Omega_1\rvert\%$	$\frac{\lvert\eta_\alpha\rvert}{\lvert J_{goal}(u_1)\rvert}$	$\frac{\lvert J_{goal}(u_1)-J_{goal}(u_\alpha)\rvert}{\lvert J_{goal}(u_1)\rvert}$	E.I.
1	0.00	$1.18 \cdot 10^{-01}$	$1.20 \cdot 10^{-01}$	0.99
2	5.00	$6.16 \cdot 10^{-02}$	$6.32 \cdot 10^{-02}$	0.97
3	15.00	$2.15 \cdot 10^{-02}$	$2.21 \cdot 10^{-02}$	0.97
4	20.02	$7.93 \cdot 10^{-03}$	$8.23 \cdot 10^{-03}$	0.96

Table 4: Predator-prey system (model adaptation): iteration, percentage of fine areas, estimator of the relative error, actual relative error, model effectivity index.

provided for a scalar nonlinear problem.

4.1 The anisotropic framework

We resort to the anisotropic setting in [22]. Let $T_K : \widehat{K} \to K$ be the invertible affine map from the reference triangle $\widehat{K}$ to the general one K, where $\widehat{K}$ is the equilateral triangle inscribed in the unit circle centered at the origin. The map T_K is defined as

$$\mathbf{x} = (x_1, x_2)^T = T_K(\widehat{\mathbf{x}}) = M_K\widehat{\mathbf{x}} + \mathbf{t}_K \quad \forall=(x_1, x_2)^T \in K, \tag{33}$$

where $M_K \in \mathbb{R}^{2\times 2}$ and $\mathbf{t}_K \in \mathbb{R}^2$ denote the Jacobian of T_K and a shift, respectively. The map T_K strains the circle circumscribed to $\widehat{K}$ into an ellipse circumscribing K, centered at the barycenter of K.
We exploit the spectral properties of T_K to describe the orientation and the shape of each K. With this aim we factorize M_K by a polar decomposition as $M_K = B_K Z_K$, where B_K is symmetric positive definite and Z_K is orthogonal. Then we further factorize B_K in terms of its eigenvalues $\lambda_{1,K}, \lambda_{2,K}$ (with $\lambda_{1,K} \geq \lambda_{2,K}$) and eigenvectors $\mathbf{r}_{1,K}, \mathbf{r}_{2,K}$, as $B_K = R_K^T \Lambda_K R_K$, with $\Lambda_K = diag(\lambda_{1,K}, \lambda_{2,K})$ and $R_K^T = [\mathbf{r}_{1,K}, \mathbf{r}_{2,K}]$.
The geometric features of each element K are thus completely characterized by the eigenvectors $\mathbf{r}_{i,K}$ and the eigenvalues $\lambda_{i,K}$, with $i = 1, 2$: as a matter of fact, they identify the directions and the lengths of the semi-axes of the ellipse circumscribing K, respectively (see Fig. 10). We measure the aspect ratio of K with respect to $\widehat{K}$ by the so-called `stretching factor` $s_K = \lambda_{1,K}/\lambda_{2,K} \geq 1$, with $s_K = 1$ whenever K is an equilateral triangle.

Starting from these decompositions, anisotropic interpolation error estimates have been derived for both the Lagrange and the Clèment interpolants ([22, 23]).

In particular, the Clément operator in [15] turns out to be prone to the a posteriori analysis below. In the case of affine finite elements, it is given by $I_h^1 : L^2(\Omega) \to X_h^1$, such that

$$I_h^1 v(\mathbf{x}) = \sum_{N_j \in \mathcal{N}_h} P_j v(N_j)\varphi_j(\mathbf{x}) \quad \forall v \in L^2(\Omega), \tag{34}$$

where φ_j is the Lagrangian basis function associated with the node N_j, $X_h^1 = \text{span}\{\varphi_j\}$, while P_j denotes the L^2-projection onto the affine functions associated with the patch Δ_j of the elements sharing node N_j, defined by the relations

$$\int_{\Delta_j} (P_j v - v)\psi \; d\Delta_j = 0 \quad \text{with } \psi = 1, x_1, x_2.$$

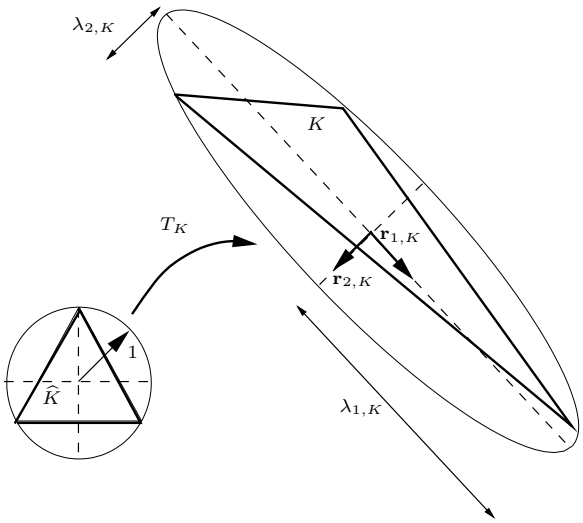

Figure 10: Geometrical interpretation of the map T_K and main anisotropic quantities.

The sum in (34) runs on the set $\mathcal{N}_h$ of the vertices of $\mathcal{T}_h$ except those where Dirichlet data are strongly enforced.

Now for any function $v \in H^1(\Omega)$, let $G_K(v) \in \mathbb{R}^{2\times 2}$ be the symmetric positive semi-definite matrix given by

$$\big[G_K(v)\big]_{i,\,j} = \int_{\Delta_K} \frac{\partial v}{\partial x_i}\frac{\partial v}{\partial x_j}\, d\Delta_K, \quad \text{with } i,j = 1,2,$$

and with Δ_K the union (patch) of all the elements sharing at least a vertex with K.
Then as proved in [22, 23], we have:

Lemma 4.1 *Let $v \in H^1(\Omega)$. Then under the assumptions that, for any K in $\mathcal{T}_h$, $\mathrm{card}(\Delta_K) \le M$ and $\mathrm{diam}(\Delta_{\widehat{K}}) \le \widehat{C}$, with $\Delta_{\widehat{K}} = T_K^{-1}(\Delta_K)$, it holds*

$$\|v - I_h^1 v\|_{L^2(K)} \;\le\; C_1 \left[\sum_{i=1}^{2} \lambda_{i,K}^2 \, \left(\mathbf{r}_{i,K}^T\, G_K(v)\, \mathbf{r}_{i,K}\right)\right]^{1/2}, \tag{35}$$

$$|v - I_h^1 v|_{H^1(K)} \;\le\; C_2 \left(\frac{h_K}{\lambda_{1,K}\lambda_{2,K}}\right) \left[\sum_{i=1}^{2} \lambda_{i,K}^2 \, \left(\mathbf{r}_{i,K}^T\, G_K(v)\, \mathbf{r}_{i,K}\right)\right]^{1/2}, \tag{36}$$

$$\|v - I_h^1 v\|_{L^2(e)} \;\le\; C_2 \left(\frac{h_e}{\lambda_{1,K}\lambda_{2,K}}\right)^{1/2} \left[\sum_{i=1}^{2} \lambda_{i,K}^2 \, \left(\mathbf{r}_{i,K}^T\, G_K(v)\, \mathbf{r}_{i,K}\right)\right]^{1/2}, \tag{37}$$

where $C_i = C_i(M, \widehat{C})$, for $i = 1, 2, 3$.

Notice the explicit dependence of these estimates on the anisotropic quantities highlighted in Figure 10. In particular, when $\lambda_{1,K} \simeq \lambda_{2,K} \simeq h_K$, that is when the triangle is equilateral, estimates (35), (36) and (37) reduce to the corresponding isotropic results in [15].

The reference patch $\Delta_{\widehat{K}}$ in Lemma 4.1 is obtained by mapping back all the elements $T \in \Delta_K$ by means of the same transformation T_K^{-1}. The hypotheses in Lemma 4.1 essentially rule out too distorted patches in the reference framework. However the anisotropic features (stretching factor and orientation) of each $T \in \Delta_K$ are not constrained by these requirements; only the variation over Δ_K of the anisotropic quantities is affected (see [34] for more details).

4.2 The anisotropic goal-oriented error estimator

We relax now the assumption made at the beginning of Section 2.1 of working on an "extra fine" computational grid in order to focus only on the model error. We allow now for the presence of a discretization error also, still controlled in the spirit of a goal-oriented analysis. This is already a long-established area of research, covering a broad range of problems and applications. The first works were developed essentially in an isotropic framework (see, e.g., [9, 26, 30, 37]), whereas, more recently, the interest has moved to an anisotropic setting (see, e.g., [16, 23, 20, 44, 25, 17, 28, 33].
Since the main objective of the present work is in model adaptation and in its interplay with mesh adaptivity, we limit the analysis below to highlighting the principal modifications to be carried out in a goal-oriented framework when interested in an anisotropic analysis. In particular, as far as the discretization error is concerned, the full results concerning the ADR problem can be found in [24, 20, 17], while an example of anisotropic output functional control for a nonlinear vector problem is provided in [33], where the incompressible Navier-Stokes equations are addressed.
The later part of this section simply supports the anisotropic a posteriori error estimate for one of the problems solved in the above test cases, with the aim of underlining the typical structure of such an anisotropic analysis. As crucial observation, notice that the model involved in the anisotropic investigation is the adapted one.

Let us consider the adapted logistic population problem. Before stating the desired result, some notation are in order. We denote by $u_{\alpha,h}$ the discrete approximation of (26), solution to the following variational problem: find $u_{\alpha,h} \in V_h \equiv X_h^1 \subset V$ s.t.

$$a(u_{\alpha,h})(w_h) + d(u_{\alpha,h})(\alpha w_h) + s_{\alpha,h}(u_{\alpha,h}, f)(w_h) = F(w_h) \quad \forall w_h \in V_h, \tag{38}$$

where the forms $a(\cdot)(\cdot), d(\cdot)(\cdot)$ and $F(\cdot)$ are defined as in (27), while $s_{\alpha,h}(\cdot)(\cdot)$ identifies a consistent stabilization term with a view to strongly advective problems. Then we define the internal and boundary residuals given by

$$\rho_K(u_{\alpha,h}) = (f + \mu\Delta u_{\alpha,h} - \mathbf{b}\cdot\nabla u_{\alpha,h} + \sigma u_{\alpha,h} - \alpha\gamma u_{\alpha,h}^2)|_K \tag{39}$$

and

$$j_e(u_{\alpha,h}) = \begin{cases} 2\Big(\lambda u_{\alpha,h} + \mu\dfrac{\partial u_{\alpha,h}}{\partial n}\Big) & \forall e \in \Gamma_D \\ 2\Big(- c_2 + \mu\dfrac{\partial u_{\alpha,h}}{\partial n}\Big) & \forall e \in \Gamma_N \\ \Big[\mu\dfrac{\partial u_{\alpha,h}}{\partial n}\Big]_e & \forall e \in \mathcal{E}_h, \end{cases} \tag{40}$$

respectively, with e a general edge of the triangulation and $\mathcal{E}_h$ the set of the internal edges of $\mathcal{T}_h$.

The main result of this section can thus be stated.

Proposition 4.1 *Let $u_\alpha \in V$ be the weak solution to the adapted primal problem (26) and $z_\alpha \in V$ be the associated dual solution for a general goal functional J_{goal}. Let $u_{\alpha,h}$ and $z_{\alpha,h} \in V_h$ be the corresponding finite element approximations associated with a SUPG stabilization scheme. Then it holds*

$$|J_{goal}(u_\alpha) - J_{goal}(u_{\alpha,h})| \leq C \sum_{K \in \mathcal{T}_h} \alpha_K R_K(u_{\alpha,h}) \omega_K(e^z_{\alpha,h}), \tag{41}$$

where $C = C(M, \widehat{C})$, $\alpha_K = (\lambda_{1,K}\lambda_{2,K})^{3/2}$,

$$\begin{aligned} R_K(u_{\alpha,h}) &= \frac{1}{(\lambda_{1,K}\lambda_{2,K})^{1/2}} \left(\|\rho_K(u_{\alpha,h})\|_{L^2(K)} \left(1 + \frac{\tau_K h_K \|\mathbf{b}\|_{L^\infty(K)}}{\lambda_{1,K}\lambda_{2,K}} \right) \right. \\ &+ \left. \frac{\|j_e(u_{\alpha,h})\|_{L^2(\partial K)}}{2} \left(\frac{h_e}{\lambda_{1,K}\lambda_{2,K}} \right)^{1/2} \right), \end{aligned} \tag{42}$$

$$\omega_K(e^z_{\alpha,h}) = \frac{1}{(\lambda_{1,K}\lambda_{2,K})^{1/2}} \left(s_K (\mathbf{r}^T_{1,K} G_K(e^z_{\alpha,h}) \mathbf{r}_{1,K}) + s_K^{-1} (\mathbf{r}^T_{2,K} G_K(e^z_{\alpha,h}) \mathbf{r}_{2,K}) \right)^{1/2},$$

with $e^z_{\alpha,h} = z_\alpha - z_{\alpha,h}$ the adapted dual discretization error.

Proof. We provide the proof of result (41) in the Appendix. □

The right-hand side of (41) still involves, via $e^z_{\alpha,h}$, the exact adapted dual solution, thus not being directly computable. To make such a quantity practical with a view to the mesh adaptation, we resort to a suitable recovery procedure. Namely, as the weights $\omega_K(e^z_{\alpha,h})$ depend on the first order partial derivative of z_α via the matrix G_K, we exploit the standard area-weighted Zienkiewicz-Zhu gradient recovery procedure ([53, 54, 46]). Hence the matrix $G_K(e^z_{\alpha,h})$ is replaced by $G^*_K(e^z_{\alpha,h})$, where

$$\left[G^*_K(e^z_{\alpha,h})\right]_{i,j} = \int_{\Delta_K} \left(\nabla^{ZZ,i} z_{\alpha,h} - \frac{\partial z_{\alpha,h}}{\partial x_i}\right)\left(\nabla^{ZZ,j} z_{\alpha,h} - \frac{\partial z_{\alpha,h}}{\partial x_j}\right) d\Delta_K, \text{ with } i,j = 1,2,$$

and where $\nabla^{ZZ} z_{\alpha,h} = \left(\nabla^{ZZ,1} z_{\alpha,h}, \nabla^{ZZ,2} z_{\alpha,h}\right)^T$ stands for the recovered gradient of $z_{\alpha,h}$.

The global estimator for the output functional discretization error $|J_{goal}(u_\alpha) - J_{goal}(u_{\alpha,h})|$ supplied from Proposition 4.1 is consequently given by

$$\eta_h = \sum_{K \in \mathcal{T}_h} \eta_{h,K}$$

where $\eta_{h,K} = \alpha_K R_K(u_{\alpha,h}) \omega^*_K(e^z_{\alpha,h})$ is the corresponding local contribution with

$$\omega^*_K(e^z_{\alpha,h}) = \left(s_K \mathbf{r}^T_{1,K} G^*_K(e^z_{\alpha,h}) \mathbf{r}_{1,K} + {s_K}^{-1} \mathbf{r}^T_{2,K} G^*_K(e^z_{\alpha,h}) \mathbf{r}_{2,K} \right)^{1/2}.$$

The local estimator $\eta_{h,K}$ enjoys the typical structure of the goal-oriented analysis, consisting of a residual associated with the primal framework and a weight

depending on the dual problem (i.e., on the target functional). The additional multiplicative coefficient α_K gathers all the area $|K|$ information, since $|K| = \lambda_{1,K}\lambda_{2,K}|\widehat{K}|$. It will play a crucial role in the anisotropic management of the mesh.
We point out that when $\lambda_{1,K} \simeq \lambda_{2,K} \simeq h_K$, estimator η_h reduces to the standard isotropic a posteriori error estimator (see, e.g., [9, 26, 38]). The added value of result (41) with respect to the isotropic analysis is the presence of anisotropic information, essentially lumped in the weights. Finally, notice that the constant C in (41) does not appear in the definition of η_h. It may be taken into account by a suitable tuning, since C depends only on quantities associated with the reference framework.

4.2.1 The mesh adaptation procedure

To turn the error estimator η_h into an actual mesh adaptation algorithm, we apply a `metric-based` adaptive procedure. The leading idea of this algorithm is to employ in a predictive fashion the estimator η_h to identify the new adapted mesh. In more detail, at the j-th iteration of such a procedure, we follow this three-step algorithm: let $\mathcal{T}_h^{(j)}$ be the previous (background) mesh. Then:

1. Solve the adapted discrete primal and dual problems;
2. build up the new metric $M^{(j+1)}$ induced by the estimator η_h;
3. construct the new mesh $\mathcal{T}_h^{(j+1)}$ matching the metric $M^{(j+1)}$.

Concerning step (2), we pursue the two standard criteria of the mesh-optimization strategy in [9], relying on equidistributing the estimator ($\eta_{h,K} = \text{const}$, for any $K \in \mathcal{T}_h^{(j+1)}$), and on minimizing the number of mesh elements for a fixed accuracy of η_h. With an eye on the structure of the element error estimator $\eta_{h,K}$, this essentially amounts to minimizing the weights with respect to the anisotropic quantities $\mathbf{r}_{1,K}$ and s_K, since the area information is compressed in α_K and $R_K(u_{\alpha,h})$ is just a pointwise value (at least for a sufficiently fine mesh). We refer to [20, 32, 17, 33] for the details of such an approach.
With reference to step (3), we exploit the `matching condition` between a metric and a mesh (see, e.g., Definition 5.1 in [33]).

5 Merging model and mesh adaptation

This section collects both the model and the discretization analyses. For this purpose, we simply exploit the straightforward splitting

$$J(u_1) - J(u_{\alpha,h}) = \underbrace{J(u_1) - J(u_\alpha)}_{\text{model error}} + \underbrace{J(u_\alpha) - J(u_{\alpha,h})}_{\text{discretization error}}.$$

This suggests the introduction of the model-discretization estimator

$$\eta_{\alpha,h} = |\eta_\alpha| + \eta_h$$

for the functional model-discretization error $|J(u_1) - J(u_{\alpha,h})|$. The actual issue is to devise a unique procedure suitably merging both the model and the mesh

spacing adaptations.
We aim at guaranteeing that the global error $|J(u_1) - J(u_{\alpha,h})|$ be within to a given tolerance τ. We consequently split τ into two contributions, a model one τ_m and a discretization one τ_d, so that

$$\tau = \tau_m + \tau_d. \tag{43}$$

In particular, to meet the global tolerance τ, we iterate until $|\eta_\alpha| \leq \tau_m$ and, simultaneously, $\eta_h \leq \tau_d$. This gives rise to the following (α, h)-`adaptive procedure`:

1. `select an initial grid` $\mathcal{T}_h^{(0)}$, `set` $j = 0$, `flag_grid` $= 0$, `and` $\alpha\big|_K = 0, \forall K \in \mathcal{T}_h^{(0)}$;
2. `solve the adapted discrete primal and dual problems;`
3. `compute the estimators` η_α, η_h `and` $\eta_{\alpha,h}$;
4. `if` $\eta_{\alpha,h} \leq \tau$ `break`
5. `for i=1,`$\mathtt{N_{max}}$
   6. `if` $|\eta_\alpha| > \tau_m$
      7. `localize` η_α `on each` $K \in \mathcal{T}_h^{(j)}$: $\eta_{\alpha,K} = \eta_\alpha\big|_K$;
      8. `if` $|\eta_{\alpha,K}| > \delta \dfrac{\tau_m}{N_h^{(j)}}$, $\alpha\big|_K \leftarrow 1$;
   9. `if` $\eta_h > \tau_d$
      10. `set flag_grid` $= 1$;
      11. `build up the metric` $M^{(j+1)}$ `induced by` η_h;
      12. `construct the new mesh` $\mathcal{T}_h^{(j+1)}$ `matching the metric` $M^{(j+1)}$;
   13. `if flag_grid` $= 1$ `interpolate` α `on` $\mathcal{T}_h^{(j+1)}$;
   14. `solve the adapted discrete primal and dual problems;`
   15. `compute the estimators` η_α, η_h `and` $\eta_{\alpha,h}$;
   16. `if` $\eta_{\alpha,h} \leq \tau$ `break`
   17. $j \leftarrow j + 1$, `flag_grid` $= 0$

   `end`

The (α, h)-`adaptive algorithm` tries to balance both sources of error through the splitting (43). The model and the discretization phases can be swapped due to the intrinsic commutativity of the algorithm. The quantities $\mathtt{N_{max}}$, δ and $N_h^{(j)}$ involved in the model step preserve exactly the same meaning as in the α-`adaptive procedure`.

5.1 Numerical validation

We complete two of the test cases used in the numerical validation of the α-`adaptive algorithm` by adding mesh adaptation.

# it	$N_h^{(j)}$	$\lvert\Omega_1\rvert\%$	$\frac{\lvert\eta_\alpha\rvert}{\lvert J_{goal}(u_1)\rvert}$	$\frac{\eta_h}{\lvert J_{goal}(u_1)\rvert}$	$\frac{\eta_{\alpha,h}}{\lvert J_{goal}(u_1)\rvert}$	$\frac{\lvert J_{goal}(u_1)-J_{goal}(u_{\alpha,h})\rvert}{\lvert J_{goal}(u_1)\rvert}$	E.I.
1	341	0.00	$2.02 \cdot 10^{+00}$	$4.06 \cdot 10^{-01}$	$2.42 \cdot 10^{+00}$	$1.79 \cdot 10^{+00}$	1.36
2	4432	5.10	$9.83 \cdot 10^{-01}$	$2.37 \cdot 10^{-02}$	$1.01 \cdot 10^{+00}$	$8.55 \cdot 10^{-01}$	1.18
3	4970	15.12	$2.26 \cdot 10^{-01}$	$2.20 \cdot 10^{-03}$	$2.28 \cdot 10^{-01}$	$1.82 \cdot 10^{-01}$	1.25
4	4970	25.13	$2.97 \cdot 10^{-02}$	$1.82 \cdot 10^{-03}$	$3.16 \cdot 10^{-02}$	$2.26 \cdot 10^{-02}$	1.39
5	4970	30.13	$7.42 \cdot 10^{-03}$	$1.44 \cdot 10^{-03}$	$8.86 \cdot 10^{-03}$	$6.42 \cdot 10^{-03}$	1.38

Table 5: ADR vs AD (model plus mesh adaptation): iteration, number of mesh elements, percentage of fine areas, estimators of the model, of the discretization and of the total relative error, actual model-grid relative error, effectivity index.

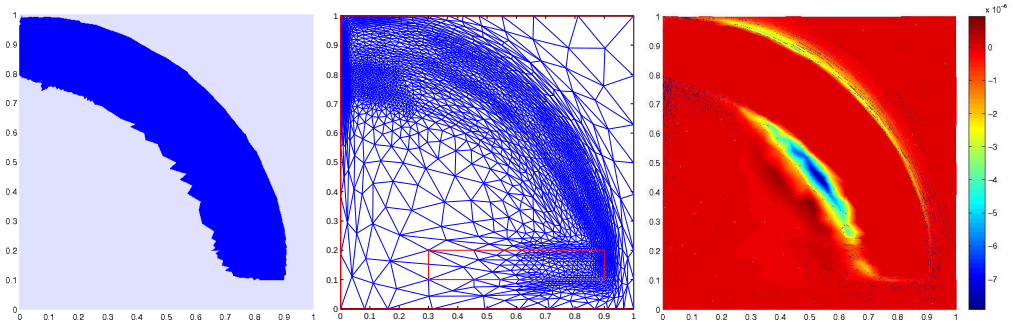

Figure 11: ADR vs AD (model plus mesh adaptation): distribution of the fine and coarse areas (left), adapted mesh (middle) and elementwise distribution of η_α (right) at the last iteration.

5.1.1 ADR versus AD

We go back to Section 2.2.1 while keeping all of the data unchanged. As supplementary information we take $\tau = 10^{-2}$, and $\tau_d = \tau_m = 0.5 \cdot 10^{-2}$. With this choice, the model-grid adaptation stops after 5 steps. In Table 5 some of the main quantities characterizing the (α, h)-`adaptive procedure` can be found. The second column keeps track of the number of mesh elements $N_h^{(j)}$; in the third column, the percentage of the whole $|\Omega|$ occupied by Ω_1 is indicated; the estimators of the model, of the discretization, and of the total relative error are provided in the fourth, fifth and sixth column, respectively; the seventh column collects the actual model-grid relative error, while in the last column we have the effectivity index E.I. $= \eta_{\alpha,h}/|J_{goal}(u_1) - J_{goal}(u_{\alpha,h})|$.
From the second column it is evident that the anisotropic mesh adaptation phase reaches quickly its target value, i.e., just at the third global iteration. Vice versa, the model adaptation lags behind, five steps being necessary to meet the exit criterion.
On comparing the sixth with the seventh column, we realize that $\eta_{\alpha,h}$ is reliable throughout all of the iterations. The robustness of the whole procedure finds a further confirmation in the values assumed by the effectivity index, always really close to 1.

Figure 11 shows the distribution of the fine and coarse areas (left), the final adapted mesh (middle), and the elementwise model estimator distribution (right) at the last iteration. The detected fine region is about 30% of the whole domain,

# it	$N_h^{(j)}$	$\lvert\Omega_1\rvert\%$	$\frac{\lvert\eta_\alpha\rvert}{\lvert J_{goal}(u_1)\rvert}$	$\frac{\eta_h}{\lvert J_{goal}(u_1)\rvert}$	$\frac{\eta_{\alpha,h}}{\lvert J_{goal}(u_1)\rvert}$	$\frac{\lvert J_{goal}(u_1)-J_{goal}(u_{\alpha,h})\rvert}{\lvert J_{goal}(u_1)\rvert}$	E.I.
1	1346	0.00	$1.27 \cdot 10^{-01}$	$1.65 \cdot 10^{-01}$	$2.91 \cdot 10^{-01}$	$1.17 \cdot 10^{-01}$	2.48
2	3891	18.38	$5.08 \cdot 10^{-02}$	$5.03 \cdot 10^{-03}$	$5.58 \cdot 10^{-02}$	$4.48 \cdot 10^{-02}$	1.25
3	4323	31.85	$1.34 \cdot 10^{-02}$	$2.84 \cdot 10^{-03}$	$1.63 \cdot 10^{-02}$	$1.30 \cdot 10^{-02}$	1.25
4	4323	40.00	$6.40 \cdot 10^{-03}$	$2.72 \cdot 10^{-03}$	$9.11 \cdot 10^{-03}$	$6.63 \cdot 10^{-03}$	1.37

Table 6: Logistic population (model plus mesh adaptation): iteration, number of mesh elements, percentage of fine areas, estimator of the model, of the discretization and of the total relative error, actual model-grid relative error, effectivity index.

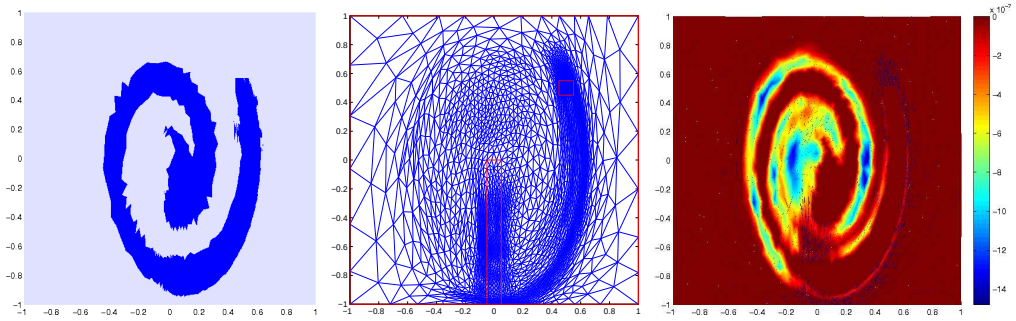

Figure 12: Logistic population (model plus mesh adaptation): distribution of the fine and coarse areas (left), adapted mesh (middle) and elementwise distribution of η_α (right) at the last iteration.

and no relevant difference can be appreciated with respect to the corresponding fine area distribution yielded by the sole model adaptation (see Fig. 2 (bottom-left)). The anisotropic features of the last adapted grid are evident. The elements align along the circular internal layer, up to the observation area. The strong refinement of the inflow can be ascribed to both the primal and dual solutions (see Fig. 1 (middle) and (right), respectively), here exhibiting sharp layers. To sum up, the zones detected as critical by both the model and discretization adaptive procedures are roughly the same. Notice that the model refinement involves a slightly smaller region. Moreover, the mesh adaptation seems to be able to identify sharper details, such as the edges on the right-hand side of the observation area. Finally, the distribution of the model error estimator in Figure 11 (right) highlights that η_α is underestimating only on a small portion of Ω.

5.1.2 The logistic population model

We enrich the analysis in Section 3.1.1 with the (α, h)-`adaptive procedure`. The total and partial tolerances are set equal to $\tau = 10^{-2}$, $\tau_d = \tau_m = 0.5 \cdot 10^{-2}$, the other data being preserved. Four iterations suffice to guarantee the desired convergence. Table 6 shares the same structure as Table 5. The mesh adaptation reaches first the corresponding tolerance, just after three iterations. On the other hand, a further step is required to guarantee the convergence of the model adaptation process. The span covered by Ω_1 at the last iteration is 40% of $|\Omega|$.

The last three columns confirm the reliability and efficiency of the estimator $\eta_{\alpha,h}$ and of the whole adaptive algorithm.

The plot on the left in Figure 12 refers to the localization of Ω_1 and Ω_0 at the last (α, h)-`iteration`. The fine area crowds around the streamlines leaving the release area E. On comparing this distribution with the one in Figure 6 (bottom-left), we observe that essentially the same zones are detected by the two adaptive procedures. The final anisotropic adapted grid in the middle of Figure 12 sharply recognizes the region more strongly affecting the fish flux across the creel, as well as a portion of the boundary of the creel itself. To a lesser extent also the remaining part of the main streamline feeding the creel is refined. The stretching factor of the elements in the circular internal layer on the right is clearly high. On the right of Figure 12, the elementwise distribution of η_α is provided. It resembles the one in Figure 6 (bottom-right). The combined effect of the model with the mesh adaptivity seems to allowing for a more loose control of the error in the areas around the fine region (compare the lighter zones in the two corresponding plots), yet guaranteeing a maximum absolute value of the order of 10^{-6}.

6 Some conclusive remarks

Results in Sections 2.2, 3.1 and 5.1 confirm the satisfactory reliability of the adaptive procedures proposed in this paper. In particular the less robust results are those related to the ADR versus DR coupling. This can be essentially ascribed to the dominant advective nature of the analyzed problems.
The investigation carried out about the interplay between model and mesh suggests that the mesh adaptation procedure is able to enrich the information provided by the model analysis with details essentially associated with geometrical or data heterogeneities.
A more thorough investigation about the model adaptivity is scheduled, also including a model coarsening step. This likely would allow us to draw more specific conclusions about the model-mesh interaction. More general nonlinear ADR systems including reactive terms different from the logistic and predator-prey models are also under study, still in an ecological-environmental setting.

Appendix. Proof of Proposition 4.1. Starting point is Proposition 2.6 in [9], according to which the discretization functional error coincides with

$$J_{goal}(u_\alpha) - J_{goal}(u_{\alpha,h}) = \min_{\phi_h \in V_h} \check{\rho}_h(u_{\alpha,h})(z_\alpha - \phi_h) + R_h, \tag{44}$$

with

$$\check{\rho}_h(u_{\alpha,h})(\cdot) = F(\cdot) - a(u_{\alpha,h})(\cdot) - d(u_{\alpha,h})(\alpha\cdot) - s_{\alpha,h}(u_{\alpha,h}, f)(\cdot),$$

$$\begin{aligned} R_h &= \widetilde{s}'_{\alpha,h}(u_\alpha, f)(z_\alpha, e^u_{\alpha,h}) - s'_{\alpha,h}(u_\alpha, f)(z_\alpha, e^u_{\alpha,h}) \\ &+ \int_0^1 \Big\{ a''(u_{\alpha,h} + se^u_{\alpha,h})(z_\alpha, e^u_{\alpha,h}, e^u_{\alpha,h}) + d''(u_{\alpha,h} + se^u_{\alpha,h})(\alpha z_\alpha, e^u_{\alpha,h}, e^u_{\alpha,h}) \\ &+ s''_{\alpha,h}(u_{\alpha,h} + se^u_{\alpha,h}, f)(z_\alpha, e^u_{\alpha,h}, e^u_{\alpha,h}) - J''_{goal}(u_{\alpha,h} + se^u_{\alpha,h})(e^u_{\alpha,h}, e^u_{\alpha,h}) \Big\} s \, ds, \end{aligned}$$

$e^u_{\alpha,h} = u_\alpha - u_{\alpha,h}$ the adapted primal discretization error and $\widetilde{s}'_{\alpha,h}(u_\alpha, f)(\cdot,\cdot)$ the stabilization term associated with the adapted dual problem, possibly coinciding only with a part of $s'_{\alpha,h}(u_\alpha, f)(\cdot,\cdot)$. By neglecting the remainder term R_h (quadratic with respect to $e^u_{\alpha,h}$) and by choosing $\phi_h = z_{\alpha,h} + I^1_h(z_\alpha - z_{\alpha,h})$, we derive from (44) the following estimate

$$J_{goal}(u_\alpha) - J_{goal}(u_{\alpha,h}) \simeq \check{\rho}_h(u_{\alpha,h})(e^z_{\alpha,h} - I^1_h e^z_{\alpha,h}).$$

Now, let us suitably rewrite the truncation error $\check{\rho}_h(u_{\alpha,h})(\phi)$, with ϕ a generic function in V. Definitions (27) combined with a SUPG stabilization (see [12]) yield

$$\begin{aligned}
\check{\rho}_h(u_{\alpha,h}) = \sum_{K\in\mathcal{T}_h} \Big\{ & \int_K \big(f\phi - \mu\nabla u_{\alpha,h}\cdot\nabla\phi - \mathbf{b}\cdot\nabla u_{\alpha,h}\phi + \sigma u_{\alpha,h}\phi - \alpha\gamma u^2_{\alpha,h}\phi\big)\, dK \\
-\lambda & \int_{\partial K\cap\Gamma_D} u_{\alpha,h}\phi\, ds - \tau_K \int_K (f + \mu\Delta u_{\alpha,h} - \mathbf{b}\cdot\nabla u_{\alpha,h} + \sigma u_{\alpha,h} - \alpha\gamma u^2_{\alpha,h})(\mathbf{b}\cdot\nabla\phi)\, dK \\
+ & \int_{\partial K\cap\Gamma_N} c_2\phi\, ds\Big\},
\end{aligned}$$

i.e., thanks to an elementwise integration by parts and to (39) and (40)

$$\check{\rho}_h(u_{\alpha,h}) = \sum_{K\in\mathcal{T}_h} \Big\{ \int_K \rho_K(u_{\alpha,h})(\phi - \tau_K\mathbf{b}\cdot\nabla\phi)\, dK - \frac{1}{2}\int_{\partial K} j_e(u_{\alpha,h})\phi\, ds\Big\}.$$

The choice $\phi = e^z_{\alpha,h} - I^1_h e^z_{\alpha,h}$ together with the anisotropic estimates in Lemma 4.1 immediately provide us with result (41).

References

[1] M. Ainsworth, *A posteriori error estimation for fully discrete hierarchic models of elliptic boundary value problems on thin domains*, Numer. Math., 80 (1998), pp. 325–362.

[2] T. Apel, *Anisotropic Finite Elements: Local Estimates and Applications*, Advances in Numerical Mathematics, Teubner, Stuttgart, 1999.

[3] I. Babuška, *The finite element method with penalty*, Math. Comput., 27 (1973), pp. 221–228.

[4] I. Babuška and W.C. Rheinboldt, *Error estimates for adaptive finite element computations*, SIAM J. Numer. Anal, 15 (1978), pp. 736–754.

[5] I. Babuška and W.C. Rheinboldt, *A posteriori error estimates for the finite element method*, Internat. J. Numer. Methods Engrg., 12 (1978), pp. 1597–1615.

[6] I. Babuška and Ch. Schwab, *A posteriori error estimation for hierarchic models of elliptic boundary value problems on thin domains*, SIAM J. Numer. Anal., 33 (1996), pp. 221–246.

[7] R.E. Bank and K. Smith, *A posteriori error estimates based on hierarchical bases*, SIAM J. Numer. Anal, 30 (1993), pp. 921–935.

[8] R.E. Bank and A. Weiser, *Some a posteriori error estimators for elliptic partial differential equations*, Math. Comp., 44 (1985), pp. 283–301.

[9] R. Becker and R. Rannacher, *An optimal control approach to a posteriori error estimation in finite element methods*, Acta Numer., 10 (2001), pp. 1–102.

[10] M. Braack and A. Ern, *A posteriori control of modeling errors and discretization errors*, Multiscale Model Simile., 1 No. 2 (2003), pp. 221–238.

[11] M. Braack and A. Ern, *Coupling multimodelling with local mesh refinement for the numerical computation of laminar flames*, Combust. Theory Model., 8 (2004), pp. 771–788.

[12] A.N. Brooks and T.J.R. Hughes, *Streamline upwind/Petrov–Galerkin formulations for convection dominated flows with particular emphasis on the incompressible Navier–Stokes equations*, Comput. Methods Appl. Mech. Engrg., 32 No. 1-3 (1982), pp. 199–259.

[13] M.J. Castro–Díaz, F. Hecht, B. Mohammadi and O. Pironneau, *Anisotropic unstructured mesh adaption for flow simulations*, Internat. J. Numer. Methods Fluids, 25 No. 4 (1997), pp. 475–491.

[14] Ph. Ciarlet, *The Finite Element Method for Elliptic Problems*, North-Holland Publishing Company, Amsterdam, 1978.

[15] Ph. Clément, *Approximation by finite element functions using local regularization*, RAIRO Anal. Numér., 2 (1975), pp. 77–84.

[16] D.L. Darmofal and D.A. Venditti, *Grid adaption for functional outputs: application to two–dimensional inviscid fluids*, J. Comput. Phys., 176 No. 1 (2002), pp. 40–69.

[17] L. Dedè, S. Micheletti and S. Perotto, *Anisotropic error control for environmental applications*, Appl. Numer. Math., 58 No. 9 (2008), pp. 1320–1339.

[18] J. Dompierre, M.-G. Vallet, Y. Bourgault, M. Fortin, and W.G. Habashi, *Anisotropic mesh adaptation: towards user-independent, mesh-independent and solver-independent CFD. III. Unstructured meshes*, Internat. J. Numer. Methods Fluids, 39 No. 8 (2002), pp. 675–702.

[19] A. Ern, S. Perotto and A. Veneziani, *Hierarchical model reduction for advection-diffusion-reaction problems*, to appear in Proceedings of ENUMATH 2007, the 7th European Conference on Numerical Mathematics and Advanced Applications, Springer-Verlag, Berlin Heidelberg, K. Kunisch, G. Of, O. Steinbach Eds. 2008.

[20] L. Formaggia, S. Micheletti and S. Perotto, *Anisotropic mesh adaptation in Computational Fluid Dynamics: application to the advection diffusion reaction and the Stokes problems*, Appl. Numer. Math. 51 (2004), pp. 511–533.

[21] L. Formaggia, F. Nobile, A. Quarteroni and A. Veneziani, *Multiscale modelling of the circulatory system: a preliminary analysis*, Comput. Visual. Sci., 2 (1999), pp. 75-83.

[22] L. Formaggia and S. Perotto, *New anisotropic a priori error estimates*, Numer. Math., 89 (2001), pp. 641–667.

[23] L. Formaggia and S. Perotto, *Anisotropic error estimates for elliptic problems*, Numer. Math., 94 (2003), pp. 67–92.

[24] L. Formaggia, S. Perotto and P. Zunino, *An anisotropic a-posteriori error estimate for a convection-diffusion problem*, Comput. Visual. Sci., 4 No. 2 (2001), pp. 99–104.

[25] E.H. Georgoulis, E. Hall and P. Houston, *Discontinuous Galerkin methods for advection-diffusion-reaction problems on anisotropically refined meshes*, SIAM J. Sci. Comput., 30 No. 1 (2007), pp. 246–271.

[26] M.B. Giles and E. Süli, *Adjoint methods for PDEs: a posteriori error analysis and postprocessing by duality*, Acta Numer., 11 (2002), pp. 145–236.

[27] W.G. Habashi, J. Dompierre, Y. Bourgault, D. Ait-Ali-Yahia, M. Fortin, M.-G. Vallet, *Anisotropic mesh adaptation: towards user-independent, mesh-independent and solver-independent CFD. I. General principles*, Internat. J. Numer. Methods Fluids, 32 No. 6 (2000), pp. 725–744.

[28] T. Leicht and R. Hartmann, *Anisotropic mesh refinement for discontinuous Galerkin methods in two-dimensional aerodynamic flow simulations*, Internat. J. Numer. Methods Fluids, 56 No. 11 (2008), pp. 2111–2138.

[29] J. L. Lions and E. Magenes, *Non-Homogeneous Boundary Value Problem and Application*, Volume I, Springer-Verlag, Berlin, 1972.

[30] Y. Maday and A.T. Patera, *Numerical analysis of a posteriori finite element bounds for linear functional outputs*, Math. Models Methods Appl. Sci., 10 (2000), pp. 785–799.

[31] G.I. Marchuk, *Adjoint Equations and Analysis of Complex Systems*, Kluwer Academic Publishers, Dordrecht, 1995.

[32] S. Micheletti and S. Perotto, *Reliability and efficiency of an anisotropic Zienkiewicz–Zhu error estimator*, Comput. Methods Appl. Mech. Engrg., 195 No. 9-12 (2006), pp. 799–835.

[33] S. Micheletti and S. Perotto, *Output functional control for nonlinear equations driven by anisotropic mesh adaption. The Navier-Stokes equations*, to appear in SIAM J. Sci. Comput. (2008).

[34] S. Micheletti, S. Perotto and M. Picasso, *Stabilized finite elements on anisotropic meshes: a priori error estimates for the advection-diffusion and Stokes problems*, SIAM J. Numer. Anal., 41 (2003), pp. 1131–1162.

[35] J.D. Murray, *Mathematical Biology. I. An Introduction*, 3rd edition, Springer Verlag, New York 2002.

[36] J.D. Murray, *Mathematical Biology. II. Spatial Models and Biomedical Applications*, 3rd edition, Springer Verlag, New York 2003.

[37] J.T. Oden and S. Prudhomme, *Goal-oriented error estimation and adaptivity for the finite element method*, Comput. Math. Appl., 41 (2001), pp. 735–756.

[38] J.T. Oden and S. Prudhomme, *Estimation of modeling error in computational mechanics*, J. Comput. Phys., 182 (2002), pp. 469–515.

[39] J.T. Oden, S. Prudhomme, D.C. Hammerand and M.S. Kuczma, *Modeling error and adaptivity in nonlinear continuum mechanics*, Comput. Methods Appl. Mech. Engrg., 190 (2001), pp. 6663–6684.

[40] J.T. Oden and K.S. Vemaganti, *Estimation of local modeling error and goal-oriented adaptive modeling of heterogeneous materials. I. Error estimates and adaptive algorithms*, J. Comput. Phys., 164 No. 1 (2000), pp. 22–47.

[41] J.T. Oden and K.S. Vemaganti, *Estimation of local modeling error and goal-oriented adaptive modeling of heterogeneous materials. II. A computational environment for adaptive modeling of heterogeneous elastic solids*, Comput. Methods Appl. Mech. Engrg., 190 No. 46-47 (2001), pp. 6089–6124.

[42] S. Oruganti, J. Shi and R. Shivaji, *Diffusive logistic equation with constant yield harvesting, I: steady states*, Trans. Amer. Math. Soc., 354 No. 9 (2002), pp. 3601–3619.

[43] S. Perotto, *Adaptive modeling for free-surface flows*, M2AN Math. Model. Numer. Anal., 40 No. 3 (2006), pp. 469–499.

[44] P.W. Power, C.C. Pain, M.D. Piggott, F. Fang, G.J. Gorman, A.P. Umpleby, A.J.H. Goddard and I.M. Navon, *Adjoint a posteriori error measures for anisotropic mesh optimisation*, Comput. Math. Appl., 52 No. 8-9 (2006), pp. 1213–1242.

[45] A. Quarteroni and A. Valli, *Domain Decomposition Methods for Partial Differential Equations*, Oxford Science Publications, New York, 1999.

[46] R. Rodriguez, *Some remark on the Zienkiewicz–Zhu estimator*, Numer. Methods Partial Differential Equations, 10 (1994), pp. 625–635.

[47] J. Shi and R. Shivaji, *Persistence in reaction diffusion models with weak Allee effect*, J. Math. Biol., 52 (2006), pp. 807–829.

[48] K.G. Siebert, *An a posteriori error estimator for anisotropic refinement*, Numer. Math. 73 No. 3 (1996), pp. 373–398.

[49] E. Stein and S. Ohnimus, *Coupled model- and solution-adaptivity in the finite-element method*, Comput. Methods Appl. Mech. Engrg., 150 (1997), pp. 327–350.

[50] E. Stein and S. Ohnimus, *Anisotropic discretization- and model-error estimation in solid mechanics by local Neumann problems. New advances in computational methods*, Comput. Methods Appl. Mech. Engrg., 176 No.1-4 (1999), pp. 363–385.

[51] R. Verfürth, *A Review of a Posteriori Error Estimation and Adaptive Mesh Refinement Techniques*, Wiley-Teubner, Chichester, 1996.

[52] M. Vogelius and I. Babuška, *On a dimensional reduction method. I. The optimal selection of basis functions*, Math. Comp., 37 (1981), pp. 31–46.

[53] O.C. Zienkiewicz and J.Z. Zhu, *A simple error estimator and adaptive procedure for practical engineering analysis*, Internat. J. Numer. Methods Engrg., 24 (1987), pp. 337–357.

[54] O.C. Zienkiewicz and J.Z. Zhu, *The superconvergent patch recovery and a posteriori error estimates. Part 1: the recovery technique*, Internat. J. Numer. Methods Engrg., 33 (1992), pp. 1331–1364.

MOX Technical Reports, last issues

Dipartimento di Matematica "F. Brioschi",
Politecnico di Milano, Via Bonardi 9 - 20133 Milano (Italy)

20/2008 F. David, S. Micheletti, S. Perotto:
Model adaption enriched with an anisotropic mesh spacing for advection-diffusion-rection systems

19/2008 S. Badia, F. Nobile, C. Vergara:
Robin-Robin preconditioned Krylov methods for fluid-structure interaction problems

18/2008 L. Bonaventura, S. Castruccio, P. Crippa, G. Lonati:
Geostatistical estimate of PM10 concentrations in Northern Italy: validation of kriging reconstructions with classical and flexible variogram models

17/2008 A. Ern, S. Perotto, A. Veneziani:
Hierarchical model reduction for advection-diffusion-reaction problems

16/2008 L. Formaggia, E. Miglio, A. Mola, A. Scotti:
Numerical simulation of the dynamics of boat by a variational inequality approach

15/2008 S. Micheletti, S. Perotto:
An anisotropic mesh adaptation procedure for an optimal control problem of the advection-diffusion-reaction equation

14/2008 C. D'Angelo, P. Zunino:
A finite element method based on weighted interior penalties for heterogeneous incompressible flows

13/2008 L.M. Sangalli, P. Secchi, S. Vantini, V. Vitelli:
K-means alignment for curve clustering

12/2008 T. Passerini, M.R. de Luca, L. Formaggia, A. Quarteroni, A. Veneziani:
A 3D/1D geometrical multiscale model of cerebral vasculature

11/2008 L. Gerardo Giorda, L. Mirabella, F. Nobile, M. Perego, A. Veneziani:
A model preconditioner for the Bidomain problem in electrocardiology